

# THERMOELECTRIC NUCLEAR FUEL ELEMENT QUARTERLY PROGRESS REPORT APRIL - JUNE 1960

By  
W. P. Blankenship  
R. C. Goodspeed  
R. A. Markley  
P. V. Mitchell

July 10, 1960

Atomic Power Department  
Westinghouse Electric Corporation  
Pittsburgh, Pennsylvania



## **DISCLAIMER**

**This report was prepared as an account of work sponsored by an agency of the United States Government. Neither the United States Government nor any agency Thereof, nor any of their employees, makes any warranty, express or implied, or assumes any legal liability or responsibility for the accuracy, completeness, or usefulness of any information, apparatus, product, or process disclosed, or represents that its use would not infringe privately owned rights. Reference herein to any specific commercial product, process, or service by trade name, trademark, manufacturer, or otherwise does not necessarily constitute or imply its endorsement, recommendation, or favoring by the United States Government or any agency thereof. The views and opinions of authors expressed herein do not necessarily state or reflect those of the United States Government or any agency thereof.**

## **DISCLAIMER**

**Portions of this document may be illegible in electronic image products. Images are produced from the best available original document.**

## LEGAL NOTICE

This report was prepared as an account of Government sponsored work. Neither the United States, nor the Commission, nor any person acting on behalf of the Commission:

A. Makes any warranty or representation, expressed or implied, with respect to the accuracy, completeness, or usefulness of the information contained in this report, or that the use of any information, apparatus, method, or process disclosed in this report may not infringe privately owned rights; or

B. Assumes any liabilities with respect to the use of, or for damages resulting from the use of any information, apparatus, method, or process disclosed in this report.

As used in the above, "person acting on behalf of the Commission" includes any employee or contractor of the Commission, or employee of such contractor, to the extent that such employee or contractor of the Commission, or employee of such contractor prepares, disseminates, or provides access to, any information pursuant to his employment or contract with the Commission, or his employment with such contractor.

This report has been reproduced directly from the best available copy.

Printed in USA. Price \$1.25. Available from the Office of Technical Services, Department of Commerce, Washington 25, D. C.

WCAP-1596  
THERMOELECTRIC NUCLEAR FUEL ELEMENT  
QUARTERLY PROGRESS REPORT - APRIL-JUNE, 1960  
CONTRACT NO. AT-(30-3)-500

July 10, 1960

G. R. Kilp, Project Engineer

W. P. Blankenship  
R. C. Goodspeed  
R. A. Markley  
P. V. Mitchell

Approved:

  
\_\_\_\_\_  
Joseph C. Danko, Manager  
Materials & Processes Section

**Westinghouse**  
ELECTRIC CORPORATION  
ATOMIC POWER DEPARTMENT  
P.O. BOX 355  
PITTSBURGH 30, PA.

TABLE OF CONTENTS

	<u>Page</u>
Summary . . . . .	1
Introduction . . . . .	2
Task 1.00 - Project Administration . . . . .	3
Task 2.00 - Fissile Thermoelectric Materials Studies . . . . .	4
Sub-Task 2.10 - Preparation of Materials . . . . .	4
Sub-Task 2.20 - Compatibility Studies . . . . .	6
Task 3.00 - Thermoelectric Measurements . . . . .	7
Task 4.00 - Irradiation Studies . . . . .	11
Task 5.00 - Design & Fabrication of Thermoelectric Nuclear Fuel Element . . . . .	16
Sub-Task 5.10 - Design of Prototype Elements . . . . .	16
Sub-Task 5.20 - Evaluation of Prototype Elements . . . . .	27
Task 6.00 - Preliminary Reactor Arrangement Studies . . . . .	29
Introduction . . . . .	29
Ground Rules . . . . .	29
Results . . . . .	30
Appendix A . . . . .	46

LIST OF FIGURES AND TABLES

	<u>Page</u>
Figure 1 - . . . . .	8
Figure 2 - . . . . .	9
Figure 3 - . . . . .	10
Figure 4 - Seebeck Coefficient of $\text{Li}_{.06}\text{Ni}_{.94}\text{C}$ as a Function of Thermal Flux . . . . .	12
Figure 5 - Resistivity of $\text{Li}_{.06}\text{Ni}_{.94}\text{O}$ as a Function of Thermal Flux .	13
Figure 6 - Seebeck Coefficient of P-Type PbTe as a Function of Thermal Flux . . . . .	14
Figure 7 - Resistivity of P-Type PbTe as a Function of Thermal Flux .	15
Figure 8 - Diametral Sizes for Swaged Thermoelectric Elements . . . .	17
Figure 9 - Section View of Prototype Element Designs . . . . .	18
Table I - Effects of Heat Treatment on Thermoelectric Properties of PbTe . . . . .	21
Table II - Compatibility Study: PbTe and GeTe with Potential Cladding Materials . . . . .	23
Figure 10 - Interface Between Fe-Al and PbTe . . . . .	24
Figure 11 - Interface Between Fe-Al and PbTe . . . . .	24
Figure 12 - Interface Between Fe-Al and PbTe . . . . .	24
Figure 13 - Interface Between Fe-Al and GeTe . . . . .	26
Figure 14 - Interface Between Fe-Al and GeTe . . . . .	26
Figure 15 - Interface Between Fe-Al and GeTe . . . . .	26
Figure 16 - Section of Single-Leg GeTe Element Tested To Failure . . .	28
Figure 17 - Case VIII Thermoelectric Fuel Element Design . . . . .	31
Figure 18 - Thermoelectric Reactor Core Thermoelectric Efficiency for Case VIII Design . . . . .	32
Figure 19 - Thermoelectric Reactor Sectional Assembly . . . . .	38
Figure 20 - Thermoelectric Reactor Core Assmby . . . . .	39
Figure 21 - Thermoelectric Reactor Cross Section . . . . .	40
Figure 22 - Thermoelectric Reactor Core Cross Section . . . . .	41
Figure 23 - Loading Estimate for Thermoelectric Reactor . . . . .	43

## SUMMARY

Necessary revisions were made to the work schedules to account for the extended shutdown at Westinghouse Testing Reactor (WTR).

A report on all materials preparation work done under the contract is nearly complete. An irradiation-testing report is in progress.

Neutron activation analysis is under consideration as a supplementary or possible replacement procedure to eliminate inconsistencies encountered in quantitative chemical analyses of the uranium compounds. New Westinghouse-purchased equipment on order or being put into service includes a 2500°C vacuum furnace, an evacuable controlled-atmosphere glove box with a gas purification system, and a digital voltmeter. A hot-pressing system and an inert atmosphere dilatometer are under construction. Two new measuring devices are in service on the testing program. Instrumentation is set up for a life-testing program.

Construction is underway on a newly-designed fission-fired thermoelectric generator. A second device, of P- and N-type PbTe, has been constructed for insertion into Experimental Test Reactor (ETR). Partial results are listed on LiNiO and on 3 M Company's PbTe.

Prototypes patterned after each of four standardized designs for swaged rod-type thermoelectric elements are being constructed and life tested. Preliminary data are presented.

Heat treat data are listed for PbTe; cold-pressing tests of PbTe and of insulating materials are described. Problems of compatibility are centered around GeTe rather than PbTe (vis-a-vis cladding materials).

From preliminary design data for a 500 KW(e) all-thermoelectric nuclear reactor core, an overall efficiency of 4.5 per cent is predicted. The figure can be raised above five per cent if makeup and dimensions of the individual thermoelectric elements are altered for the best match with local conditions in the reactor core. Design features of the reactor include light water moderation and cooling; thermal circulation of primary coolant; and an in-core assembly of 100,000 tubular-shaped series-type P- and N- PbTe junctions mounted 50 each on two thousand 40-inch-long fuel rods and connected to give 160v-3200amp D.C. output.



## INTRODUCTION

This quarterly report covers the technical progress made during the first three months of a work program developed for the period April 1, 1960 to September 30, 1960. The roster of work tasks has been expanded to include the new Task No. 6.00, Preliminary Reactor Arrangement Studies.

The irradiation testing program on thermoelectric materials has been delayed due to an unforeseen shutdown by the Westinghouse Testing Reactor (WTR). Consequently, arrangements are in progress to shift part of the proposed irradiation test programs to the Experimental Test Reactor (ETR) at the Atomic Energy Commission reactor at Arco, Idaho. The balance of the irradiation program will be conducted at WTR when operation is resumed there.

TASK 1.00 - PROJECT ADMINISTRATION

The necessary revisions of the new work program covering the period April 1, 1960 to September 30, 1960 were completed. Due to lack of progress caused primarily by the prolonged unscheduled shutdown of WTR, a new work schedule was prepared for the second half of the work period.

A trip to the Atomic Energy Commission - New York Operations Office was made by Westinghouse Atomic Power Department personnel to discuss the technical progress of the current work program.

A topical report covering previous work done under Contract No. AT(30-3)500 on preparation of mixed-valence thermoelectric compounds is nearly complete. A second topical report covering the total irradiation testing program to date is in progress.

In addition to the above topical report and two monthly reports, a quarterly report was prepared and general supervision of the project was carried out under this task.

TASK 2.00 - FISSILE THERMOELECTRIC MATERIALS STUDIES

Sub-Task 2.10 - Preparation of Materials

A serious problem has arisen in the process of developing thermoelectrically optimum compositions from among the uranium sulfides, selenides, tellurides, and ternary compositions. On the basis of all data evaluated, the results of most of the chemical analyses performed on the uranium compounds are inconsistent with the X-ray diffraction results and with the general range of results which were anticipated in each case. Briefly, the situation is as follows:

1. In the preparation of  $UX_2$  compounds, where X represents S, Se, or Te, the details of the process are such that any variation from stoichiometry must almost of necessity be in the direction of decreasing anion content; that is, the end product should be  $UX_n$  with  $n \leq 2$ .
2. This contention is firmly supported by the results of X-ray diffraction analyses, which indicate that all constituents present in the  $UX_n$  compounds contain  $n \leq 2$ .
3. In most cases, however, the results of quantitative chemical analyses indicate that  $n \geq 2$ . Furthermore, in ternary compounds  $UX_mY_n$ , where the starting materials contain  $m + n \leq 2$ , chemical results have indicated  $m + n$  values from 2.3 to 3.5.

The effects of this uncertainty on the program are threefold:

1. Obviously, adjusting composition to obtain optimum thermoelectric properties is impossible unless reliable and accurate quantitative analyses can be performed on each sample prepared.
2. Determination of the effects of doping levels and of off-stoichiometry on thermoelectric properties is equally dependent upon precise analyses.
3. A rigorous series of compatibility studies should not be initiated until a good approximation of the compositions of greatest interest, along with their most efficient operating temperatures, is obtained.

The chemical analysis of this type of compound is generally conceded to be a very difficult procedure, and the chemists at all of the analytical facilities at our disposal are reluctant to guarantee consistently reliable results. Because of this, it has been decided that neutron activation analysis, a process involving short-time neutron irradiation of the sample followed by a scanning of the resultant gamma-ray spectrum, is necessary to obtain the needed information. The present plan is to send representative samples to either Tracerlab, Inc. or to the WTR for activation analysis, and use their results as a basis for improving the chemical analysis procedure. If the chemical process continues to yield unsatisfactory results, however, it will be necessary to use the activation technique for all future analyses on the uranium chalcogenides.

A set of tantalum reaction bombs is ready for the first series of melting studies. The first materials to be prepared by melting will be  $US_2$ ,  $U_3S_5$ ,  $U_2S_3$ ,  $US$ ,  $USTe$ ,  $US_{0.5}Te_{0.5}$ , and  $USe$ .

A new furnace has been ordered which will provide operating temperatures up to  $2500^{\circ}C$  in vacuum. It will be used as a high-temperature heat treating furnace, and as a heat source for those bomb melting experiments which require temperatures in excess of  $2000^{\circ}C$  ( $US$ ,  $U_2S_3$ ,  $USe$ ,  $UTe$ , and possibly some of the ternary compositions).

A completely new hot-pressing system has been designed and is nearly constructed. The new unit will provide a higher quality inert atmosphere and better control of hot-pressing parameters, and it will be easily adaptable for experiments such as bomb melting at temperatures up to  $2000^{\circ}C$ .

The inert-atmosphere dilatometer is now being calibrated; the first series of thermal expansion measurements on the uranium compounds will be made during the next report period. It is hoped that this data will also yield information on solid-state phase transformations and thermal stability of the uranium compounds at temperatures up to  $1000^{\circ}$ - $1100^{\circ}C$ .

A new, evacuable controlled-atmosphere glove box and a gas purification system have been ordered. These will be used in the preparation,

handling, and storage of the uranium compounds. It is expected that the high-quality inert atmosphere to be provided by this system will assure greatly-improved purity of the uranium-compound powders, and thus result in improved thermoelectric properties and more precisely evaluable materials.

A procedure is being designed for the preparation of uranium sulfide and of pure, finely-divided uranium powder from uranium hydride ( $\text{UH}_3$ ). Numerous references cite the decomposition of  $\text{UH}_3$  as an excellent method for obtaining uranium metal in a highly reactive form. It is anticipated that the use of uranium in this form for preparation of sulfides, selenides, and tellurides will alleviate most of the diffusion problems encountered in the use of uranium shavings.

#### Sub-Task 2.20 - Compatibility Studies

As indicated under Sub-Task 2.10, a formal program for this topic will not be prepared until the chemical analysis situation is resolved.

### TASK 3.00 - THERMOELECTRIC MEASUREMENTS

During this quarter, several new pieces of measuring equipment have been procured. The most important and versatile of these is a KIN TEL Digital Voltmeter System (Figure 1). This system accepts up to 200 D.C. voltages, measures them sequentially, and prints out on paper tape the following information:

1. channel being measured
2. polarity
3. location of the decimal point
4. five significant figures

The accuracy is plus or minus one digit in the fifth significant figure with a resolution of one microvolt. Auxiliary equipment has been built to provide a time signal to one of the channels and to periodically apply D.C. power to heaters and resistivity measuring circuits. It is planned to use this digital voltmeter to automatically monitor all experiments on a round-the-clock basis.

Two new measuring devices have also been constructed and are being prepared for service. One is designed to measure Seebeck coefficients, resistivities, and bond resistances of swaged and machined thermoelectric wafers. The other device (Figure 2) is designed to measure all three thermoelectric parameters of cylindrical thermoelectric pellets at temperatures up to  $1000^{\circ}\text{C}$ . If this device performs as expected, materials of construction for a later version will be selected to provide for higher operating temperatures.

All instrumentation for a life testing program has been set up for swaged samples of lead tellurides. Since these samples are completely encapsulated, they may be operated at temperatures approaching the melting point without subliming. Two types of samples have been prepared. The first consists of a single leg of P- or N-type material and the second consists of a complete couple of P- and N-type materials. Figure 3 is a photograph of a P- and N-type PbTe couple in the as-machined condition, ready for instrumentation. The details of the fabrication of these samples are reported under Sub-Task 5.10.

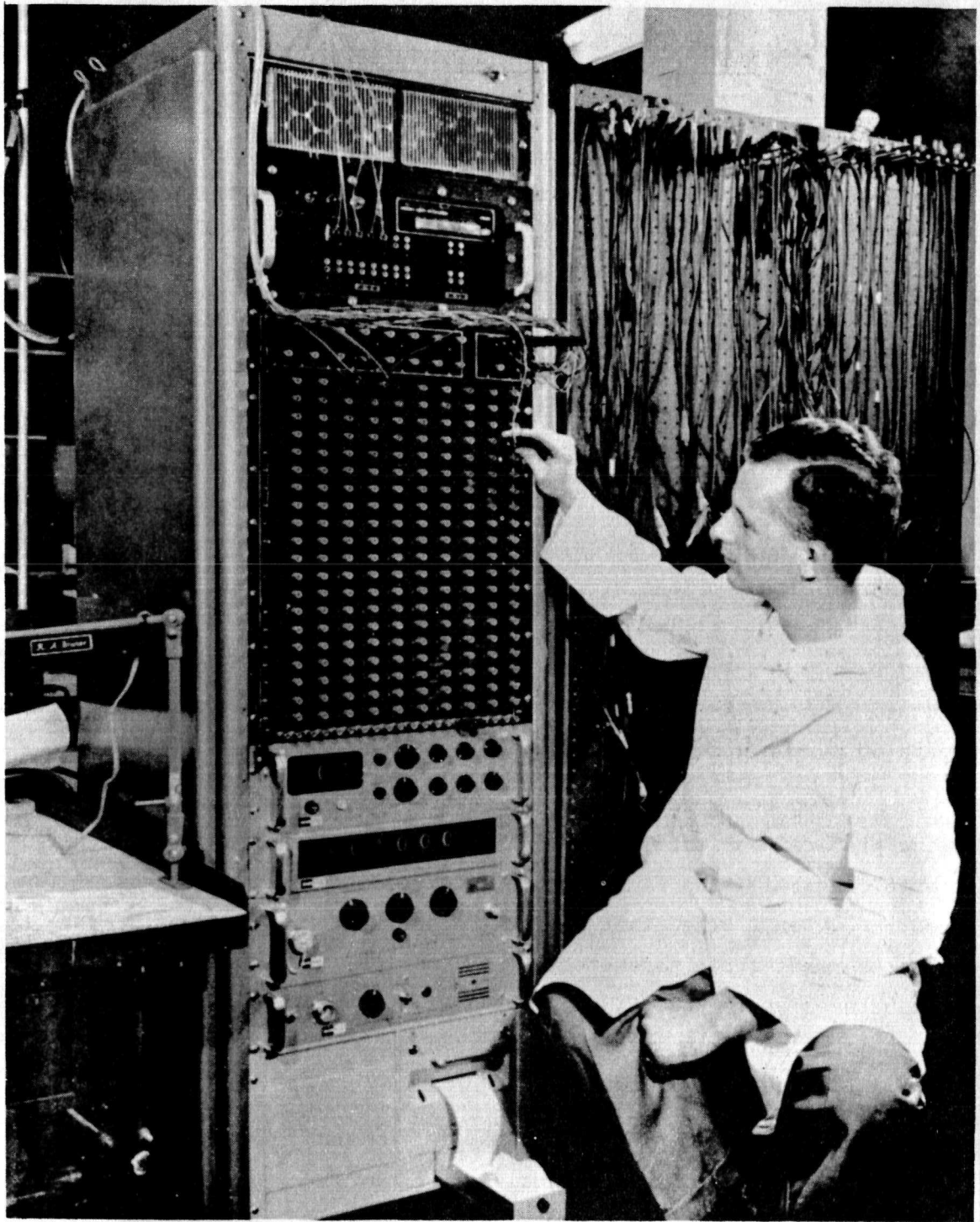


FIGURE 1



FIGURE 2



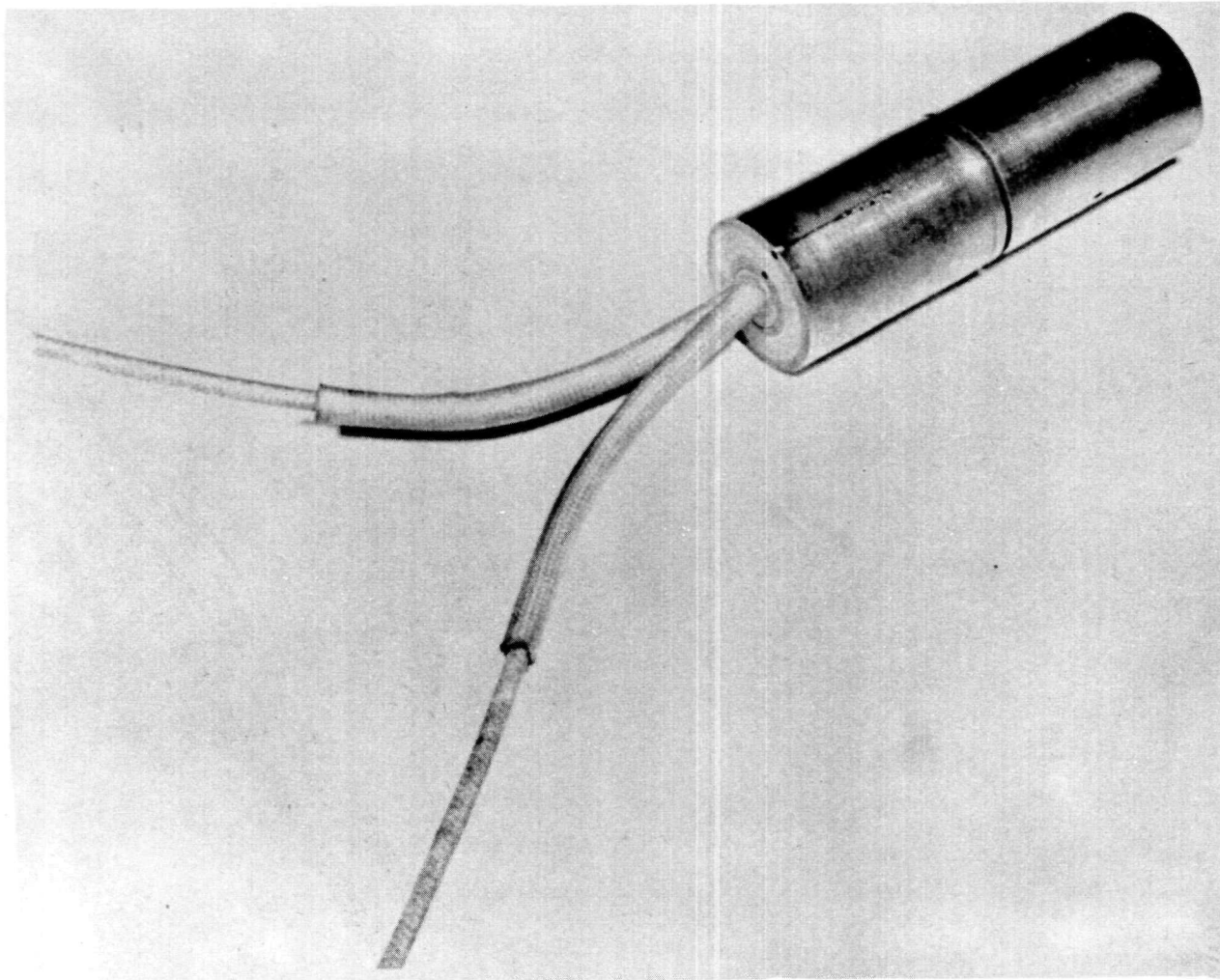


FIGURE 3

#### TASK 4.00 - IRRADIATION STUDIES

Since WTR has been out of operation, no experiments were performed there this quarter. However, the design of a fission-fired thermoelectric generator has been completed, and construction has begun. It is planned to insert this experiment as soon as WTR resumes operation.

An uninstrumented capsule containing P- and N-type PbTe has been constructed for insertion in ETR in the near future. These samples are to be used in isothermal annealing studies. An instrumented sample of swaged PbTe is also planned for ETR.

An analysis of the in-pile experiment performed last quarter at Brookhaven National Laboratories (BNL) has been completed. Both samples were exposed to an integrated flux of approximately  $10^{19}$  nvt. The  $\text{Li}_{.06}\text{Ni}_{.94}\text{O}$  sample was run at an average temperature of  $400^{\circ}\text{C}$  with a  $\Delta T$  of approximately  $50^{\circ}\text{C}$ . Neither the Seebeck coefficient nor the electrical resistivity changed from their pre-irradiation values of  $175 \mu\text{v}/^{\circ}\text{K}$  and  $0.016 \text{ ohm-cm}$ , respectively, as shown in Figures 4 and 5.

The P-type 3 M PbTe was run at an average temperature of  $375^{\circ}\text{C}$  and a  $\Delta T$  of approximately  $50^{\circ}\text{C}$ . The data, plotted in Figures 6 and 7, shows that the Seebeck coefficient has increased only slightly, but the resistivity has doubled and shows no tendency to saturate. This behavior is surprising since the damage should anneal at a temperature well below the operating temperature of the sample. The changes in the Seebeck coefficient and the resistivity are consistent with a change in the concentration of the doping agent (Na) from 0.3 atomic per cent to 0.1 atomic per cent. A similar increase in resistivity with time at elevated temperature has been observed in laboratory tests. Thus the resistivity change is probably due to a loss of doping agent rather than to any radiation effect.

The last in-pile experiment to be performed at BNL is being prepared. This will consist of two additional  $\text{Li}_x\text{Ni}_{1-x}\text{O}$  samples to fill in the gap in the range of compositions previously studied.

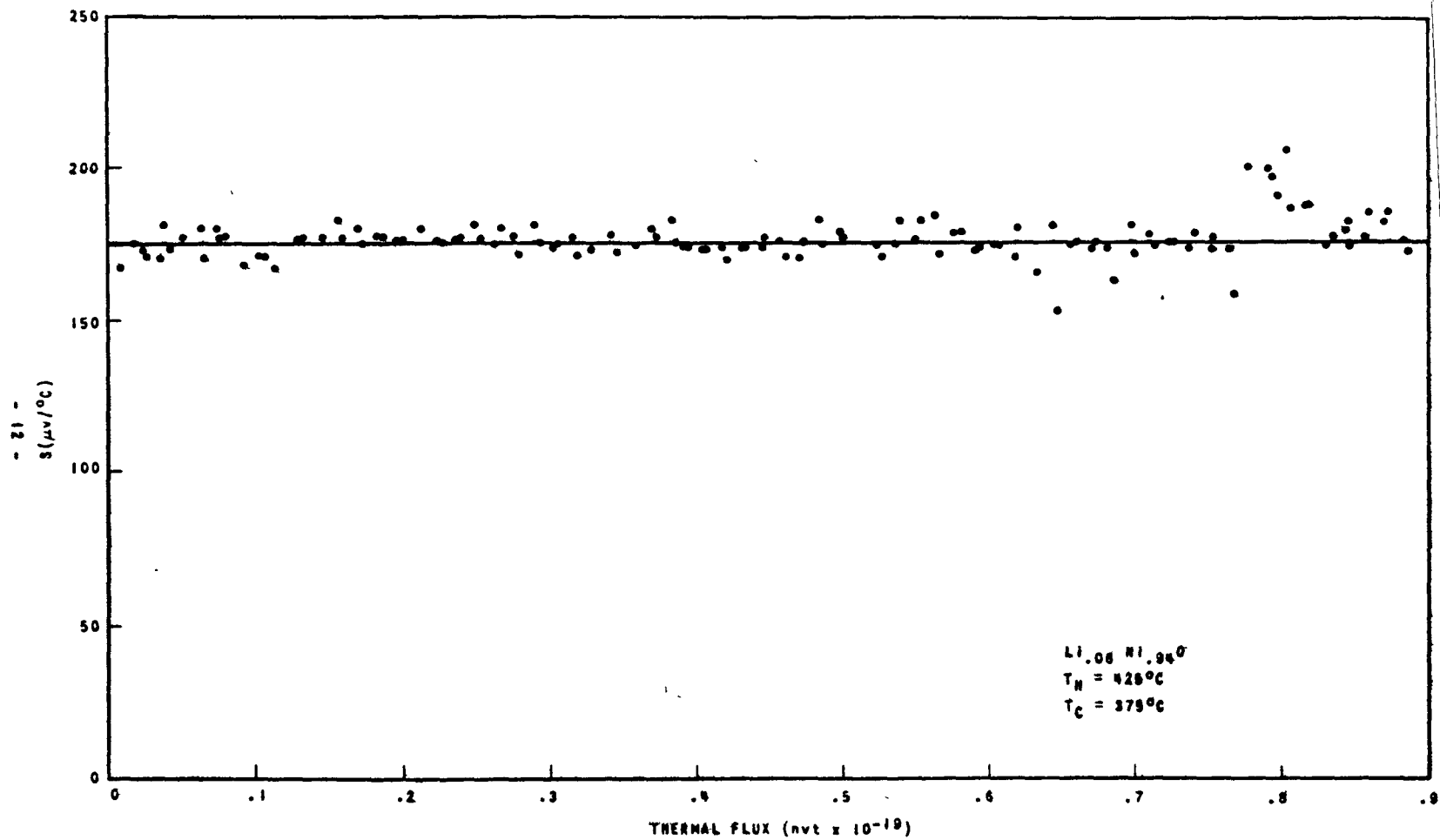


FIGURE 4  
 SEEBECK COEFFICIENT OF  $\text{Li}_{0.06}\text{Ni}_{0.94}\text{O}$  AS A FUNCTION OF THERMAL FLUX

ED. SK. 288800 C

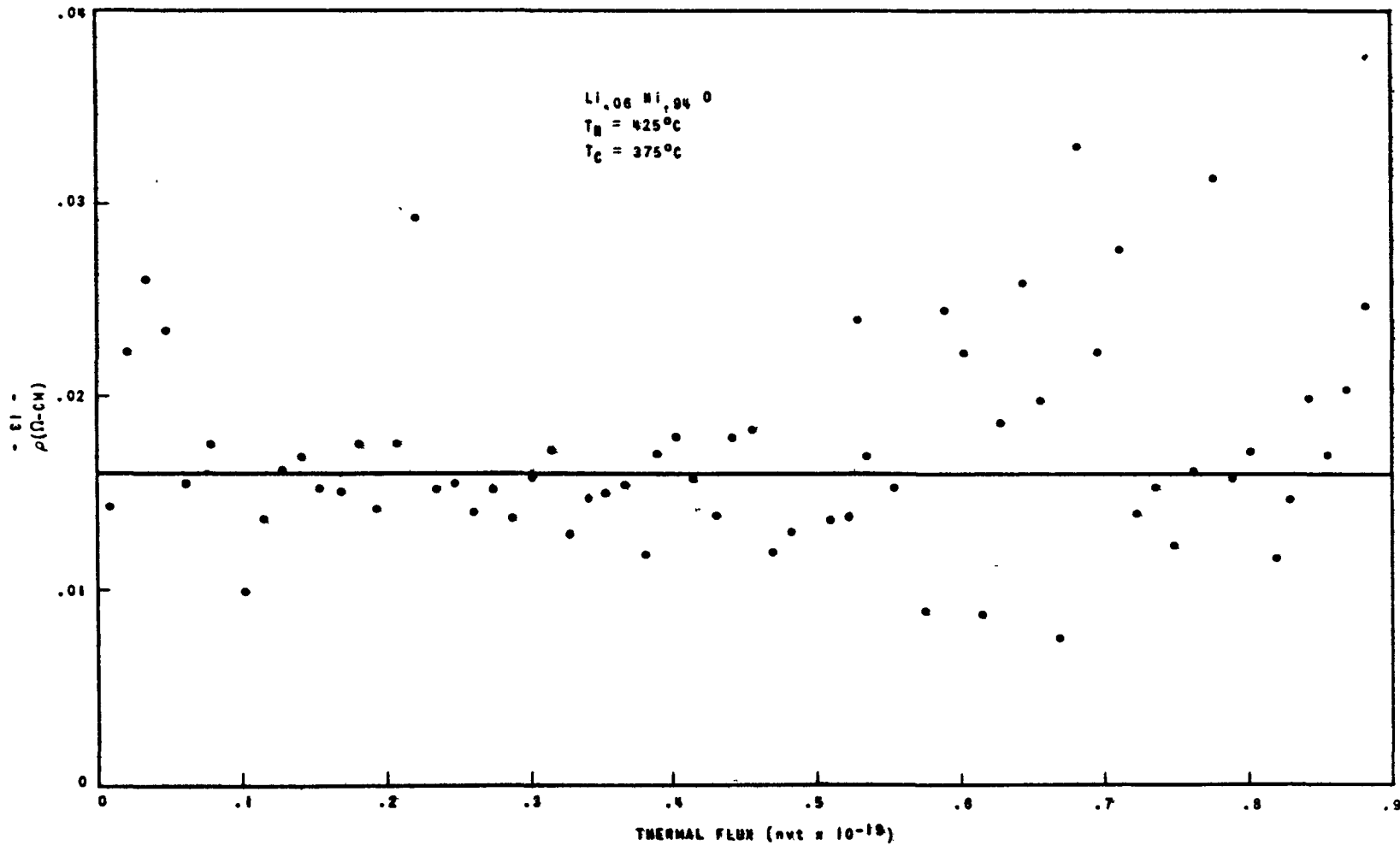


FIGURE 5  
 RESISTIVITY OF  $\text{Li}_{0.06}\text{Ni}_{0.94}\text{O}$  AS A FUNCTION OF THERMAL FLUX

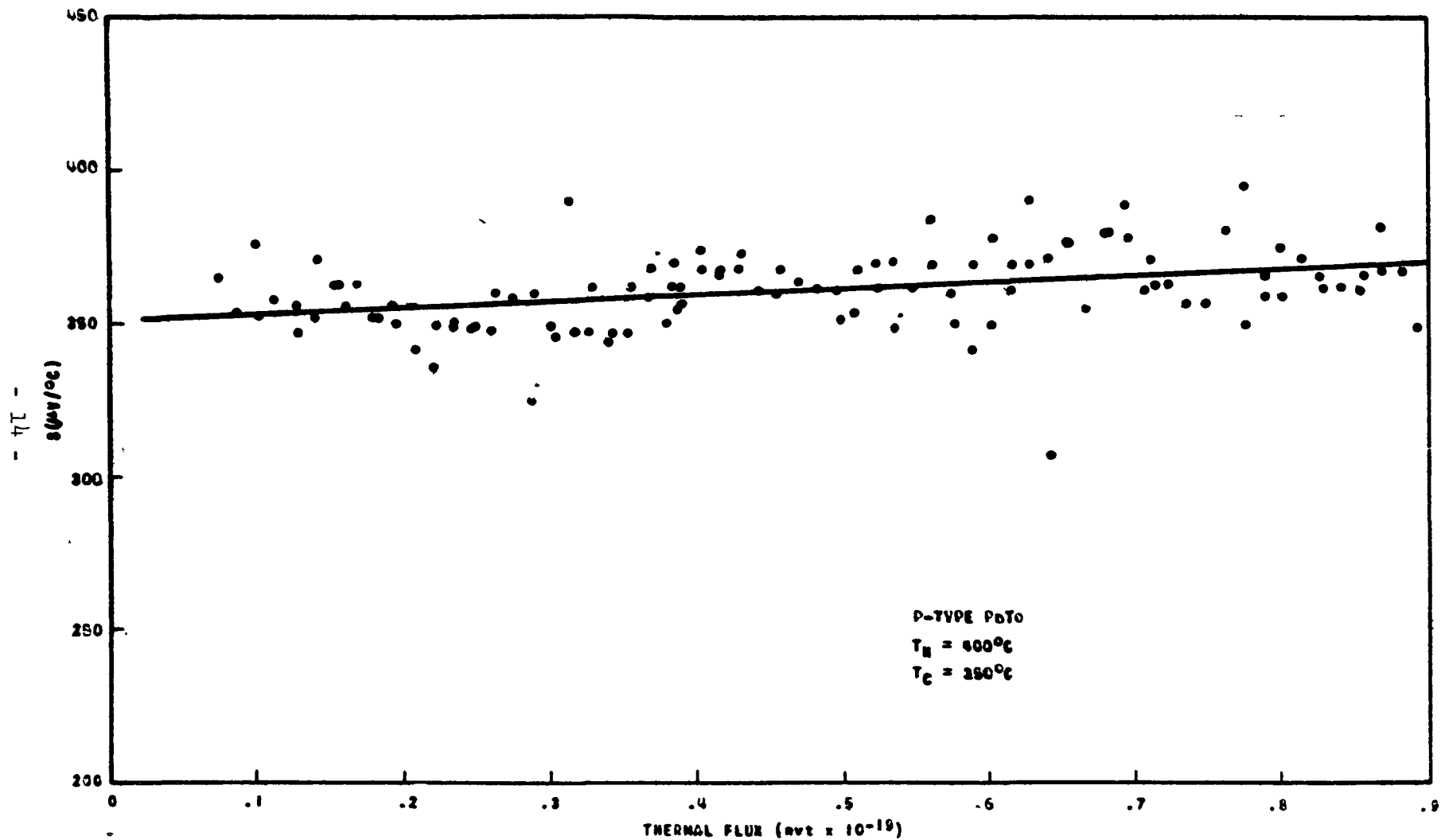


FIGURE 6

SEEBECK COEFFICIENT OF P-TYPE PbTe AS A FUNCTION OF THERMAL FLUX

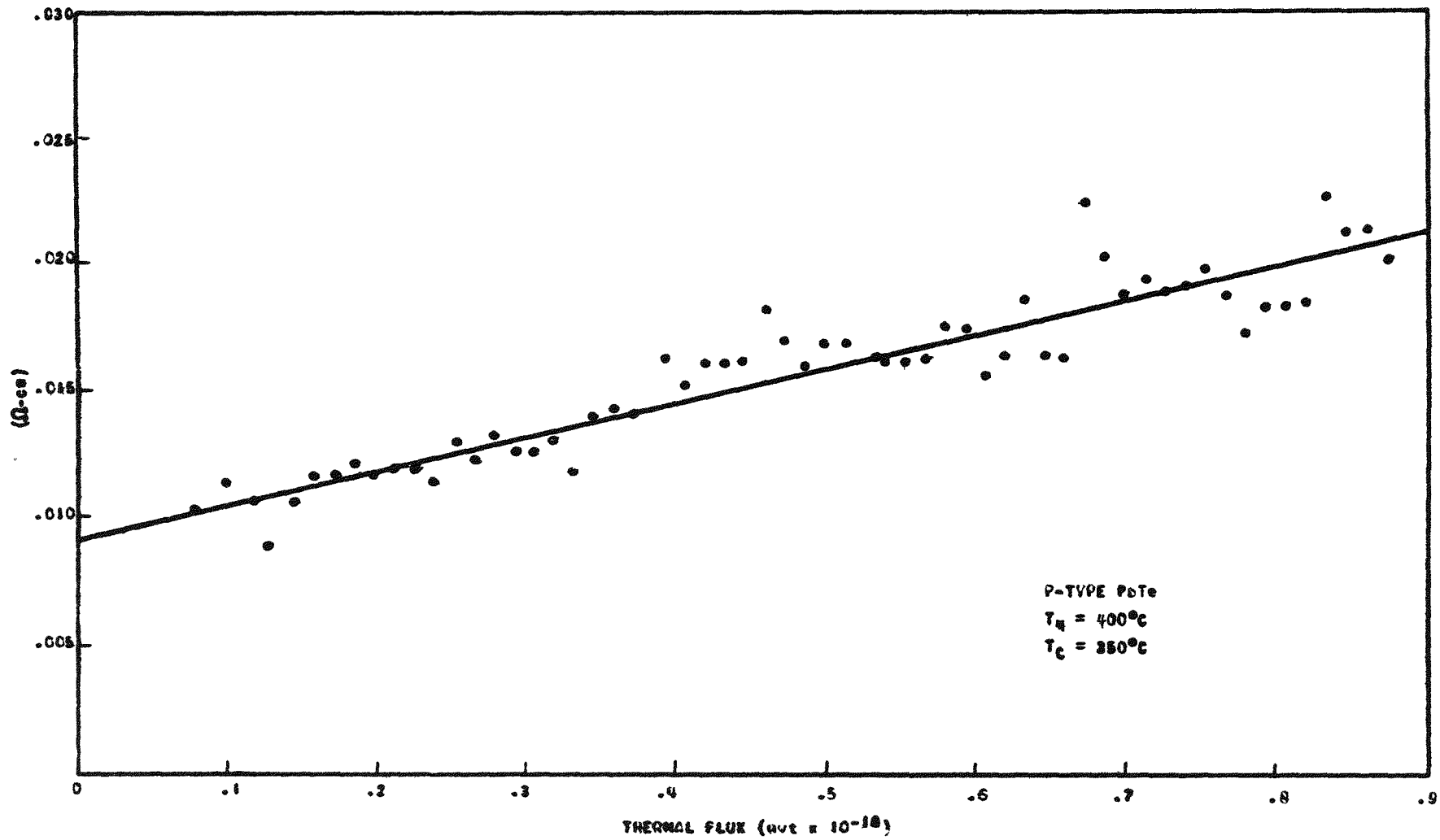


FIGURE 7

RESISTIVITY OF P-TYPE PbTe AS A FUNCTION OF THERMAL FLUX

## TASK 5.00 - DESIGN & FABRICATION OF THERMOELECTRIC NUCLEAR FUEL ELEMENT

Design, fabrication, and evaluation of rod-type thermoelectric elements have been expanded in a fundamental direction. The current work program may be divided into five general phases:

- A. Standardization of dimensions and element designs.
- B. Fabrication of prototype elements (by swaging) for testing of fabrication techniques and thermoelectric properties.
- C. Supporting studies on (1) the cold-pressing and heat-treating of thermoelectric and insulating materials, (2) the compatibility of thermoelectric materials with cladding materials, and (3) fabrication techniques.
- D. Testing and evaluation of prototype elements.
- E. Metallurgical examination of elements which have failed.

### Sub-Task 5.10 - Design of Prototype Elements

- A. A set of element dimensions and several of the more useful element designs have been standardized.

The dimensions (Figure 8) were carefully computed to allow each of the several elements to be easily fabricated, correctly instrumented (with center heat source and with current, potential, and thermocouple leads), and readily tested by insertion into the 1.000 inch in-pile test capsule.

Four element designs have been chosen as likely to provide the most useful data:

1. The single-leg design (Figure 9a) for providing scientific data (viz., Seebeck EMF, electrical resistivity, and thermal conductivity of the specific material being tested).
2. The double-leg design (Figure 9b) for providing engineering data (viz., total Seebeck EMF's and resistivities, and average thermal conductivities of the two materials being tested).

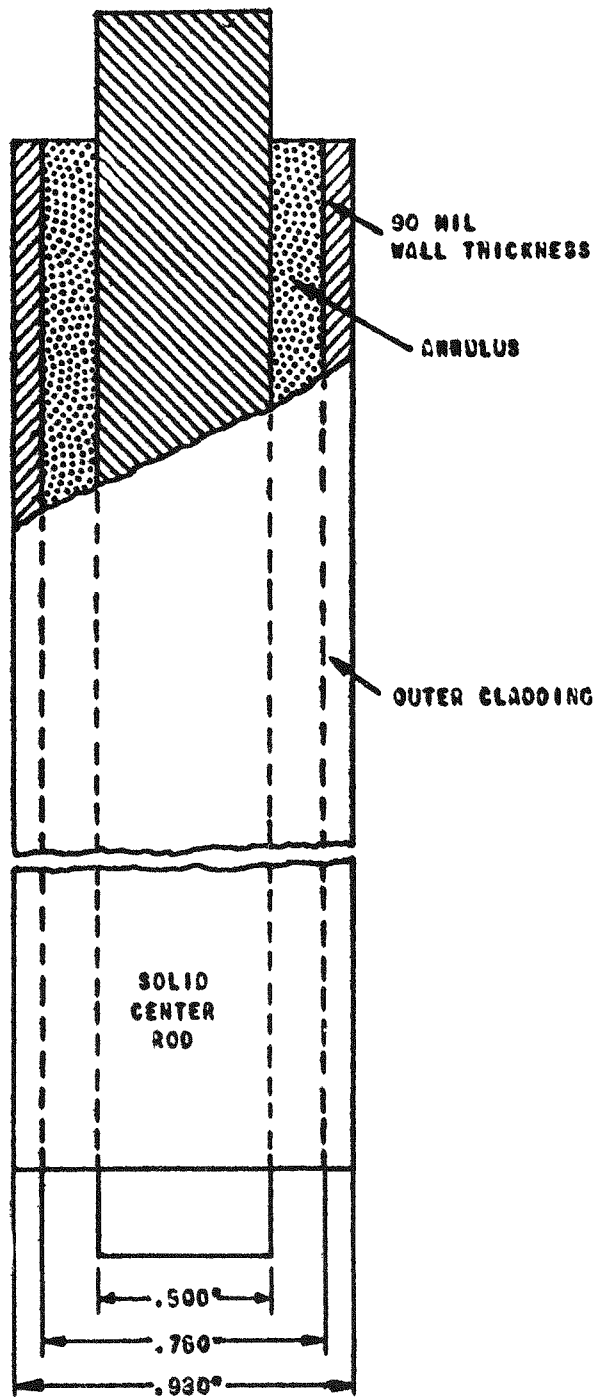
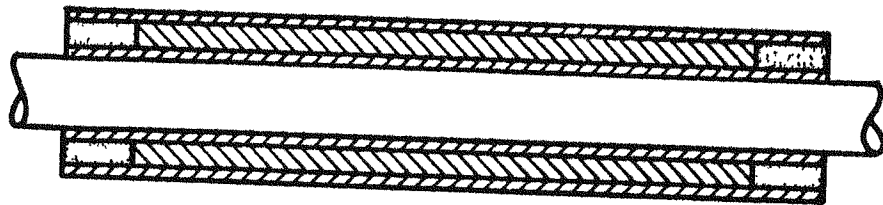
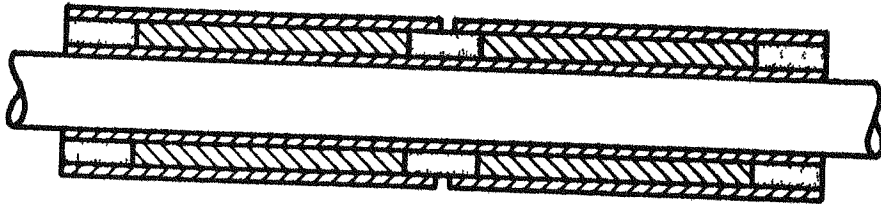


FIG. 8 DIAMETRAL SIZES FOR SWAGED THERMOELECTRIC ELEMENTS

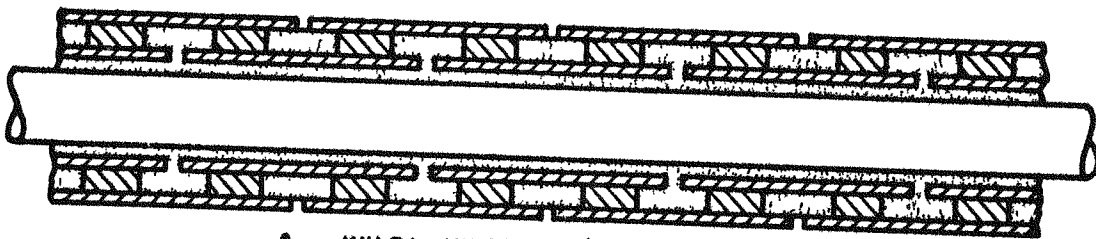




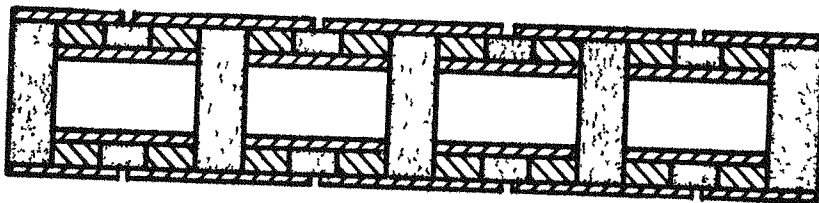
A - SINGLE LEG



B - DOUBLE LEG



C - MULTI-JUNCTION (NOTCHED BAR)



D - MULTI-JUNCTION (PELLETIZED)

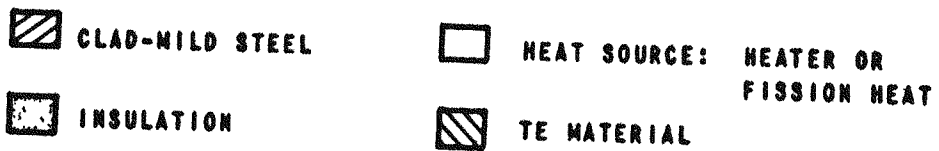


FIGURE 9  
SECTION VIEW OF PROTOTYPE ELEMENT DESIGNS

ED. Sk. 288835 C

3. The multi-junction, notched-bar design (Figure 9c) for providing useful power.
4. The multi-junction, pelletized design (Figure 9d) for providing useful power.

Of the two multi-junction element designs, the pelletized one is considerably easier to fabricate. All four designs will provide life expectancy data.

B. Prototypes of each design are completed or nearly so. Four three-inch-long single-leg elements were identically loaded with finely powdered PbTe, two with 78.8 grams of the N-type and two with 78.8 grams of the P-type. All were swaged to 0.930 inch O.D. and are being instrumented with a heat source and with current, potential, and thermocouple leads. They will be heat-treated for six hours at 600°C in a helium atmosphere, and life tested.

Two three-inch-long double-leg elements were also identically loaded with powdered PbTe. In each element, the loading in one leg was 35.3 grams of the N-type and in the other, 35.3 grams of the P-type. One element was then cold-swaged to 0.930 inch O.D. and heat-treated for six hours at 600°C before machining for instrumentation. The second was cold-swaged to 0.980 inch O.D. (to completely seal it), heat-treated approximately sixteen hours at 600°C, cooled to 300°C, hot-swaged to 0.930 inch O.D., and annealed for six hours at 600°C before machining for instrumentation. Both elements are now being tested.

Several prototypes of the multi-junction elements are presently being fabricated, mainly for evaluation of new fabrication techniques rather than for construction of test specimens.

C. New supporting studies have been initiated and current ones continued in the more fundamental fields of:

1. Properties of thermoelectric and insulating materials.
2. Compatibility of thermoelectric materials with potential cladding materials.
3. Fabrication of elements by swaging.

The subjects covered in the fundamental property studies are the cold pressing of thermoelectric and insulating materials; the effects of heat treating on the thermoelectric properties of finely powdered thermoelectric materials; and the effects of heat-treating on cut and pressed insulating materials.

Cold pressing data were obtained for N-type PbTe, P-type PbTe, a lavite powder, and mica powder. The percentages of theoretical density resulting from the cold pressing were plotted versus the respective pressing pressures for the several materials. In all cases, the green density was found to increase with increasing pressure for a constant amount of material, and to remain constant with various amounts of material at a constant pressure. A die for the pressing of annular rings of thermoelectric materials was designed, ordered, and received. Insulating materials are also being pressed in this die, but these powders display an undesirably high recovery upon ejection.

The effects of heat-treatment on the thermoelectric properties of pressed pellets of finely powdered thermoelectric materials have been studied to aid in optimization of element loading and fabricating (Table I). Four pellets were pressed from finely-ground N-type PbTe, one immediately after grinding and one each after 24, 48, and 120 hour delays. The initial (as-pressed) room temperature resistivities of the pellets generally increased as the delay between the actions of crushing and pressing was lengthened, probably due to a progressive buildup of oxide film on the particles. Subsequent sintering of the pellets resulted in room temperature resistivities which were uniformly low, suggesting that the oxide buildup was readily dissolvable in the sintering process. The highest Seebeck coefficient obtained for each of the four pellets was in the range 235 to 275  $\mu\text{v}/^{\circ}\text{C}$ , about 100  $\mu\text{v}/^{\circ}\text{C}$  higher than the initial values. The test data did not supply information as to the optimum operating values for the  $T_H$ ,  $T_C$ , and the  $\Delta T$  for the N-type PbTe.

Similar data are presented in Table I for P-type PbTe. Again, (a) the as-pressed room temperature resistivities of the pellets increased as the post-grinding delays were lengthened from 0 to 24 to 48 to 144 hours,

TABLE I

EFFECTS OF HEAT TREATMENT ON THERMOELECTRIC PROPERTIES OF PbTe

<u>Sample Parameters</u>				<u>Room Temperature Resistivities, Seebeck Coefficients,</u>				<u>Temperature</u>		
<u>Delay Between Grinding and Pressing of Powder, (hrs.)</u>	<u>As-Pressed Density, Per Cent of Theoretical</u>	<u>Pellet Dimensions, (inch)</u>		<u>ohm-cm x 10<sup>-3</sup></u>		<u><math>\mu\text{v}/^{\circ}\text{C}</math></u>		<u>Data for Maximum Seebeck</u>		
		<u>Diameter</u>	<u>Length</u>	<u>Pre-Sinter</u>	<u>Post-Sinter</u>	<u>Minimum (Pre-Sinter)</u>	<u>Maximum (During Sintering)</u>	<u>T<sub>H</sub>, °C</u>	<u>T<sub>C</sub>, °C</u>	<u>ΔT, °C</u>
<u>N-Type</u>										
0	96.8	0.523	0.575	86	1.6	134	235	446	238	208
24	96.5	0.523	0.578	53	0.5	153	273	563	446	117
48	97.0	0.523	0.578	197	1.1	124	251	676	387	289
120	96.5	0.523	0.582	139	0.7	152	240	513	201	380
<u>P-Type</u>										
0	96.7	0.523	0.591	5	0.6	145	288	455	195	260
24	95.7	0.523	0.598	8	0.8	122	298	502	235	267
48	97.6	0.523	0.587	13	2.2	122	279	500	209	291
144	95.2	0.523	0.602	27	9.0	132	291	484	257	227

and (b) subsequent sintering of these P-type pellets resulted in room temperature resistivity values much lower than the as-pressed values. In contrast to the result for the N-type, however, there was a marked trend toward higher values for those pellets pressed after the longer post-grinding delays. The maximum Seebeck coefficients were all in the range 280 to 300  $\mu\text{v}/^\circ\text{C}$ , this time about 150  $\mu\text{v}/^\circ\text{C}$  higher than the initial values. The optimum values for  $T_H$ ,  $T_C$ , and  $\Delta T$  were found to be in the ranges 460-500 $^\circ\text{C}$ , 200-250 $^\circ\text{C}$ , and 230-290 $^\circ\text{C}$ , respectively.

Further data will be obtained from each of the eight pellets after a 600 $^\circ\text{C}$  sintering for six hours in a helium atmosphere.

The study of the effects which various heat-treatments exert upon insulating materials was initiated because of observed warpage of a swaged element upon annealing. Such warpage, if due to expansion of the insulating washers, may cause separation of the thermoelectric materials from the clad, thus resulting in failure by open circuit.

Expansion data (per cent volume change versus time at 600 $^\circ\text{C}$ ) are being obtained for cut lavite, uncontained pressed lavite, contained pressed lavite, cut Mycalex, uncontained pressed mica, and contained pressed mica. The data are not yet ready for presentation.

The study of compatibility of PbTe and GeTe with potential cladding materials was continued. New cladding materials have been tested (or are being tested) at 510 $^\circ\text{C}$ , 600 $^\circ\text{C}$ , and 650 $^\circ\text{C}$ . These materials include an Fe - 7 w/o Al alloy, an Fe - 7 w/o Al - 4.3 w/o Cr alloy, and ferritic stainless steel. Also, the temperature range of testing of materials previously investigated has now been extended from 510 $^\circ\text{C}$  to 700 $^\circ\text{C}$  (see Table II).

PbTe proved to be compatible with both the Fe - 7 w/o Al and Fe - 7 w/o Al - 4.3 w/o Cr alloys at temperatures up to 650 $^\circ\text{C}$  and for times up to 200 hours (Figures 10, 11, and 12).

TABLE II

COMPATIBILITY STUDY: PbTe AND GeTe WITH POTENTIAL CLADDING MATERIALS

Temperature, °C	510			600			650			700		
Hours at Temperature	200	2	40	200	1	100	200	1	20	100		
PbTe with												
Molybdenum							x		y	y		
Niobium		x	x		x	x	x		y	y		
Zircaloy-2		x	x		x	x	x		y	y		
1100 Aluminum		x	x		x	x	x		y	y		
304 Stainless Steel							x		y	y		
Low Carbon Steel		x	x		x	x	x		y	y		
Fe - 7 w/o Al	---	z	z	.15 mil	z	.25 mil	.25 mil					
Fe - 7 w/o Al - 4.3 w/o Cr	.25 mil	z	z	.15 mil	z	z	.25 mil					
Ferritic Stainless Steel		y	y	y								
GeTe with												
Molybdenum			y		x	x	x		y	y	y	
Tungsten			y				x		y	y	y	
Zircaloy-2			y		x	x	x		y	y	y	
1100 Aluminum			y				x		y	y	y	
304 Stainless Steel		x	x	x	x	x	x		y	y	y	
Low Carbon Steel			y		x	x	x		y	y	y	
Fe - 7 w/o Al	.7 mil	1 mil	5 mils	20 mils	6 mils	c	c		-	-	-	
Fe - 7 w/o Al - 4.3 w/o Cr	.5 mil	.6 mil	5 mils	16 mils	4 mils	c	c		-	-	-	
Ferritic Stainless Steel		y	y	y								

x - Reported in WCAP-1545 - Thermoelectric Nuclear Fuel Element Quarterly Progress, Jan.-March, 1960

y - Heat-treated, but not mounted

z - No reaction occurred

c - Samples reacted catastrophically

Mil values are widths of reaction zones in thousandths of an inch

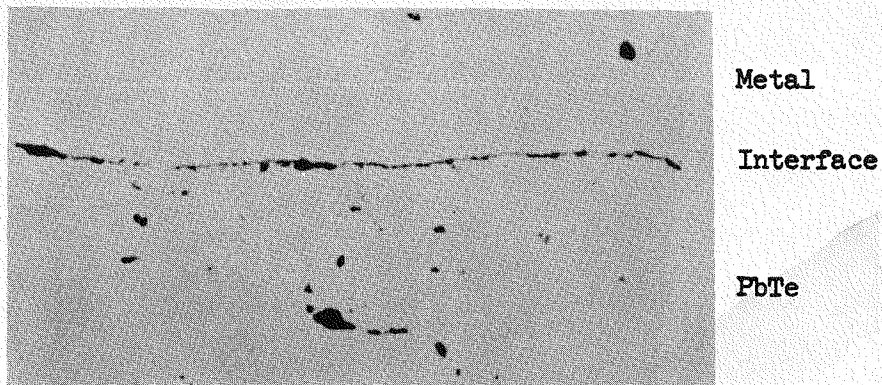


FIGURE 10 - Interface between Fe-7 w/o Al and PbTe -  
510°C for 200 hours 250X

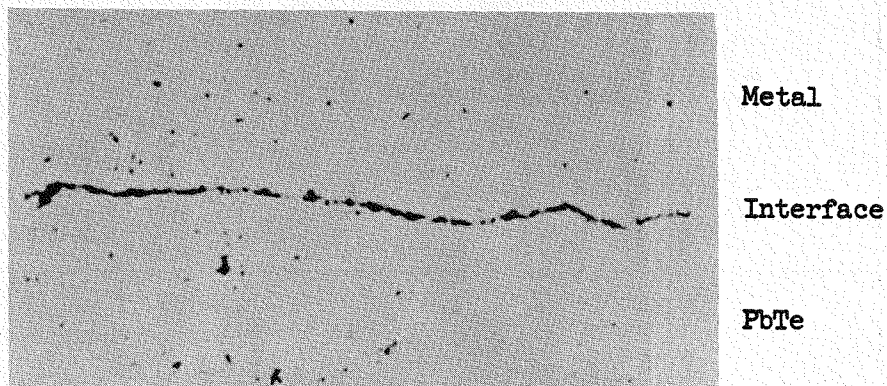


FIGURE 11 - Interface between Fe-7 w/o Al and PbTe -  
600°C for 200 hours 250X

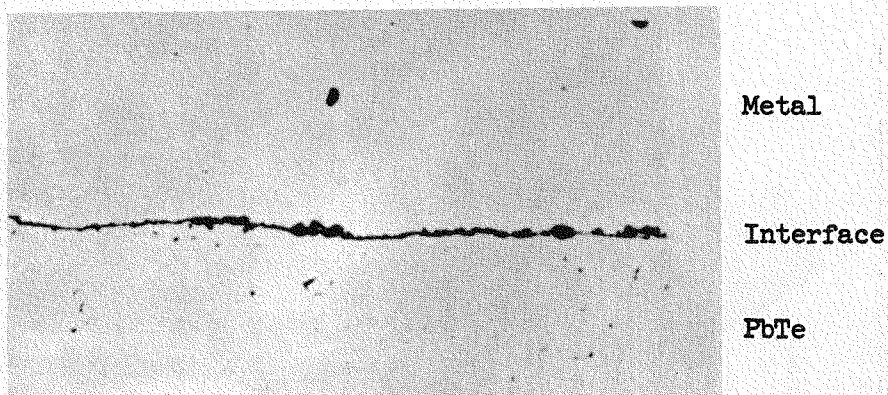


FIGURE 12 - Interface between Fe-7 w/o Al and PbTe -  
650°C for 200 hours 250X

Only quite minor, localized chemical reaction, if any, can be observed in most of the tested samples. Since the two alloys were equally compatible with the PbTe, a photograph of only one is shown as representative of both.

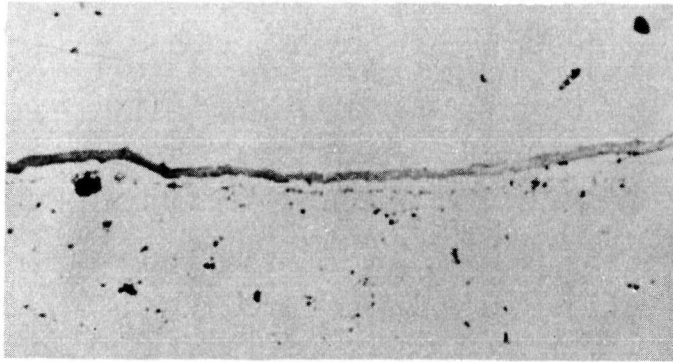
GeTe, on the other hand, reacted catastrophically with both alloys in 200 hours at 600°C, and in only a few hours at 650°C. Again, test results from only one alloy are shown (Figures 13, 14, and 15). The outside cladding in Figures 14 and 15 is mild steel. Note the extent of reaction with the GeTe.

Future work will be directed towards finding a satisfactory (and thus far elusive) cladding material that is compatible with GeTe. Chromium and vanadium will be among the materials tested.

Swaging was further studied as a fabrication process for the manufacture of thermoelectric elements. A close examination of X-ray photographs of all the swaged elements revealed several significant results. In every case, the dimensions in the as-swaged condition had turned out to be gratifyingly close to the standardized dimensions (Figure 8). This was particularly true when the thermoelectric loading density was high (about 90 per cent of theoretical) and the swaging was light. Even the dimensions of the hot-swaged double-leg element (previously mentioned) were extremely close. Since the loadings and the final swaged dimensions were identical for the two double-leg elements, the swaging temperature, below 300°C, apparently has little effect on the as-swaged density of either N- or P-type PbTe.

However, it was found that the swaging temperature does have an effect on the uniformity of the diameter of the center rod and on the wall thickness of the clad. Examinations of the X-ray photographs revealed that a more uniform wall thickness of the clad and a much less uniform diameter of the center rod resulted from hot swaging. These phenomena were believed to result from the quenching effect of the swaging dies on the clad surface during hot swaging. An X-ray indication that hot swaging increases fracturing in the insulating material will be investigated.





Metal

Two-Zone Interface

GeTe

**FIGURE 13** - Interface between Fe-7 w/o Al and GeTe -  
510°C for 200 hours 250X

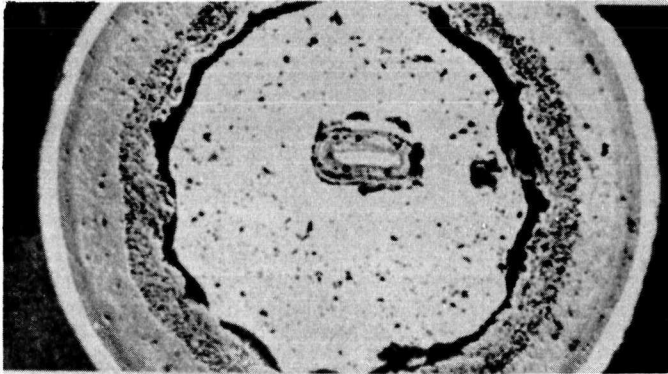


**FIGURE 14** - Interface between Fe-7 w/o Al and GeTe -  
600°C for 200 hours 8X

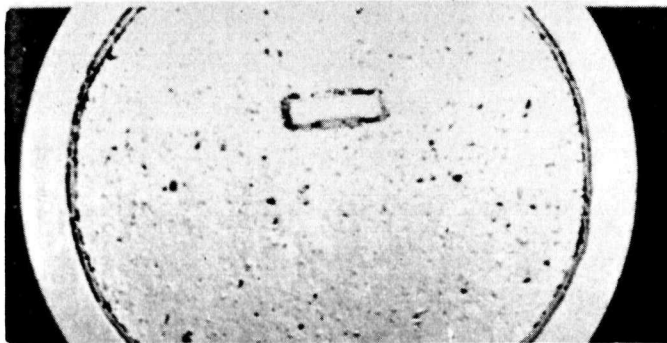


**FIGURE 15** - Interface between Fe-7 w/o Al and GeTe -  
650°C for one hour 8X

## Sub-Task 5.20 - Evaluation of Prototype Elements

D. The four single-leg elements and the two double-leg elements are now being life tested or are being instrumented for life testing. The hot junctions will be maintained at temperatures somewhat below the melting point of the PbTe ( $922^{\circ}\text{C}$ ), but not below  $600^{\circ}\text{C}$ . The cold junctions will be water cooled to maintain them near room temperature, or (to allow good control of the temperature drop across the thermoelectric material) the elements will be placed in a furnace to operate at higher temperatures. The life tests will be continuously monitored by the digital voltmeter described under Task 3.00 - Thermoelectric Measurements. On an appropriate schedule of regular intervals, the elements' outputs (D.C. voltage and amperage, the latter as measured across a standard load resistor) and the hot- and cold-junction temperatures (thermocouple EMF's) will be recorded to five significant figures.

Several multi-junction elements will be fabricated shortly for life testing.

E. Final results were tabulated on the first element to be life tested. It was a swaged, single-leg GeTe element. Failure occurred after a total of 115 days of testing with hot-junction temperatures of about  $320^{\circ}\text{C}$  for the first 44 days and of  $580\text{-}600^{\circ}\text{C}$  for the last 71 days.\* During the first testing period, both the resistivity and the Seebeck EMF remained remarkably constant. In the second period, however, the resistivity increased greatly. While the Seebeck EMF decreased, its change was much less radical than had been that of the resistivity.

A section from the element after failure was metallographically polished and examined (Figure 16). Reaction zones at both of the austenitic stainless steel clad - GeTe interfaces were about 0.025 inch thick. These reaction zones, if found to be of higher electrical resistance than the GeTe, would account for the increased resistivity and the decreased Seebeck EMF noted above for this element.

---

\* There was an axial temperature gradient in the element as well as a radial one. The cold-junction temperatures were about 40 degrees below the hot-junction temperatures.

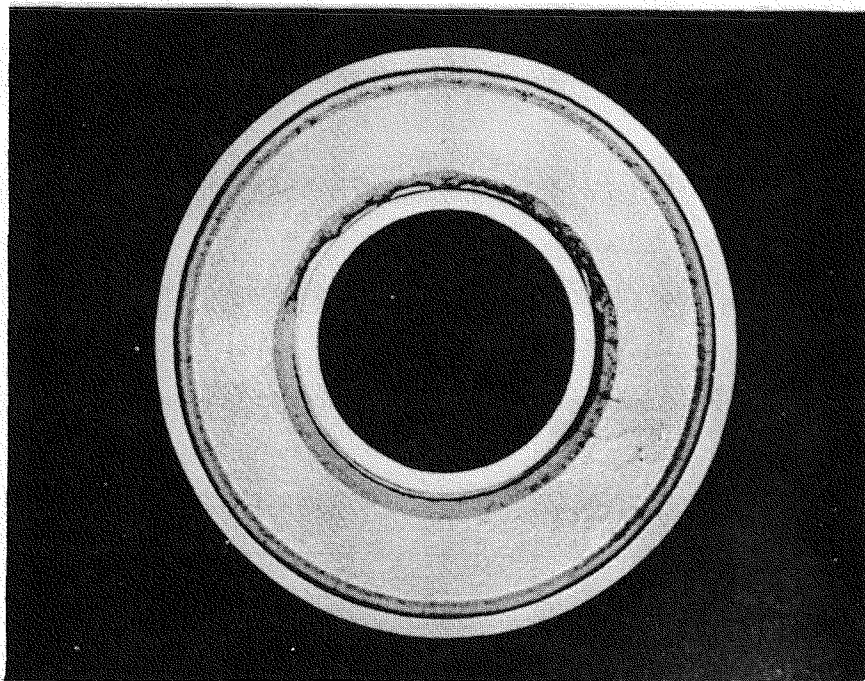


FIGURE 16 - Section of single-leg GeTe element tested to failure - shows clad-GeTe interfaces 4X

## TASK 6.00 - PRELIMINARY REACTOR ARRANGEMENT STUDIES

### Introduction

Work was initiated on preliminary reactor arrangement studies. The objectives of this investigation are:

1. To conceive and optimize the design of workable thermoelectric nuclear reactor cores.
2. Evaluate the feasibility and performance of these cores for producing power.

This study would entail investigating the electrical, mechanical, hydraulic, thermal, nuclear physics, material, and controls performance of any such reactor core for proper operation and power conversion. Performance, reliability, life, and control must be thoroughly considered to make such an evaluation.

### Ground Rules

The following "Ground-Rules" were established for a first approach at a thermoelectric reactor system design:

1. Utilization of a light-water-moderated-and-cooled nuclear reactor core.
2. Production of all electrical power directly from thermoelectric material, so that no external power conversion equipment (turbine-generator sets) will be required.
3. Production of 500 KW(e) of D.C. power in the reactor.
4. Utilization of thermal circulation of the coolant in the primary system.
5. Adoption of in-core series-type junctions with the thermoelectric material "wrapped around" the nuclear fuel element.
6. Utilization of PbTe with P and N doping agents as the thermoelectric material.

Some additional "preferred" criteria are:

1. Highest attainable efficiency
2. Low pressure system
3. High voltage output to reduce power transmission losses.
4. High reliability
5. Simplicity and compactness
6. Long life at top performance

The product of these rules would be a compact, reliable, simple, integral nuclear reactor system which would produce 500 KW(e) D.C. power and a large quantity of heat from an integral heat exchanger for utilization as process or space heat. Such a system requires no pumps in the primary coolant circuit, and eliminates turbine-generator sets with all their auxiliary equipment.

It should be noted that electrical outputs much smaller than the specified 500 KW(e) are equally feasible and may be developed if the applications exist.

Various schemes for the placement of the thermoelectric material in the unit appear worth consideration. The thermoelectric material may be located either within or external to the reactor core, or may be combined in the same reactor system. If located within the core, the radial temperature gradient may be utilized to obtain the required  $\Delta T$  across a thermoelectric element.

## Results

### A. Thermoelectric Core Characteristics

Figure 17 shows the rod-type fuel element chosen as a basis for the preliminary reactor arrangement studies. Figure 18 is a plot of the thermoelectric efficiencies (as calculated by the "average parameter"<sup>1</sup> method) versus the design figure of merit ( $S_j^2/K_j R_j$ ), where

---

<sup>1</sup> "Calculation of Efficiencies of Thermoelectric Devices," B. Sherman, R. R. Heikes, and R. W. Ure, Jr., Westinghouse Research Laboratory, Journal of Applied Physics, Vol. 31, No. 1, January, 1960, pp. 1-16. See also the "exact" and "infinite staging" methods. The extra time these methods would require to achieve accuracy only 5 to 10 per cent greater was not felt warranted for this preliminary effort.

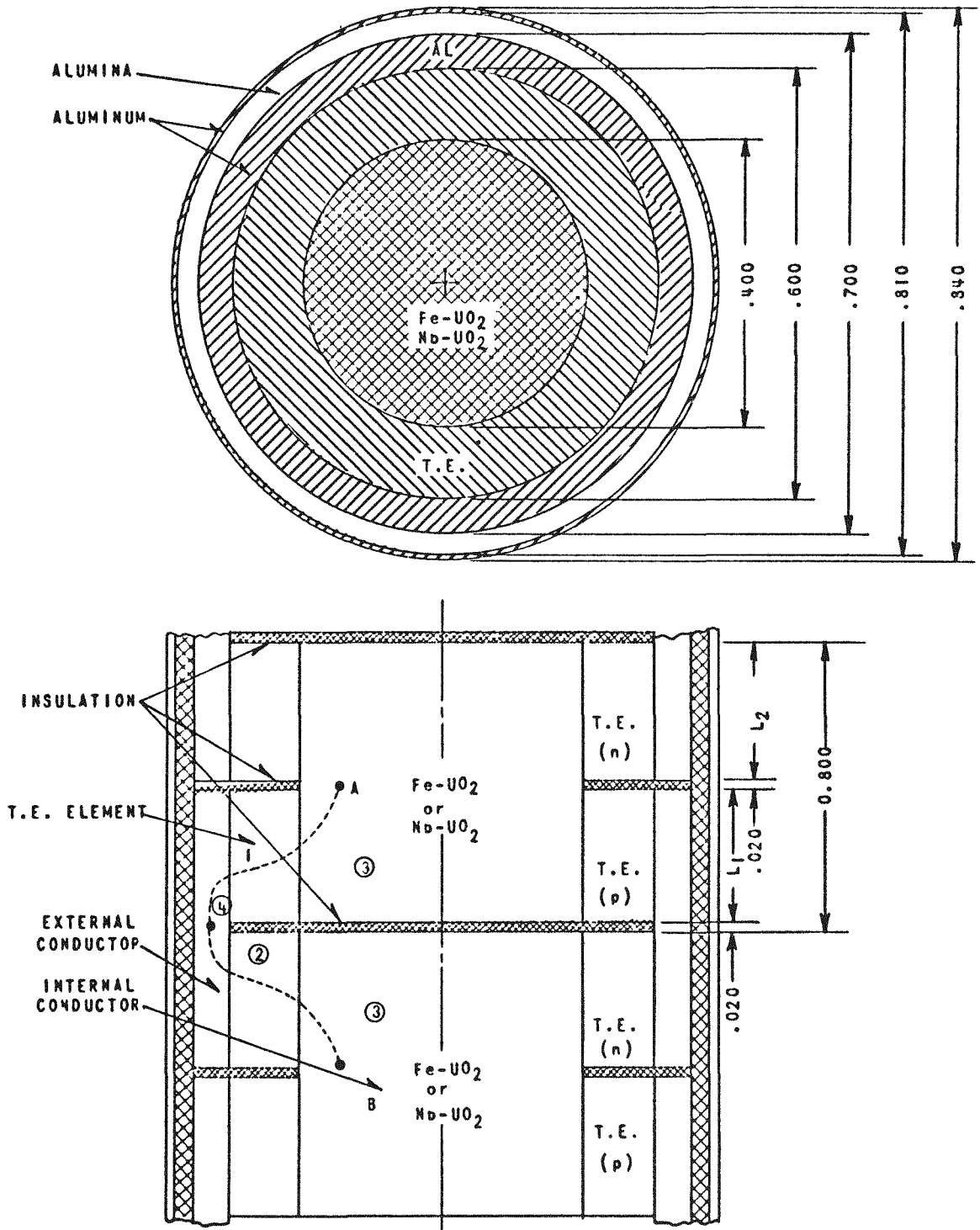


FIG. 17  
CASE VIII T.E. FUEL ELEMENT DESIGN

ED. Sk. 288735 C

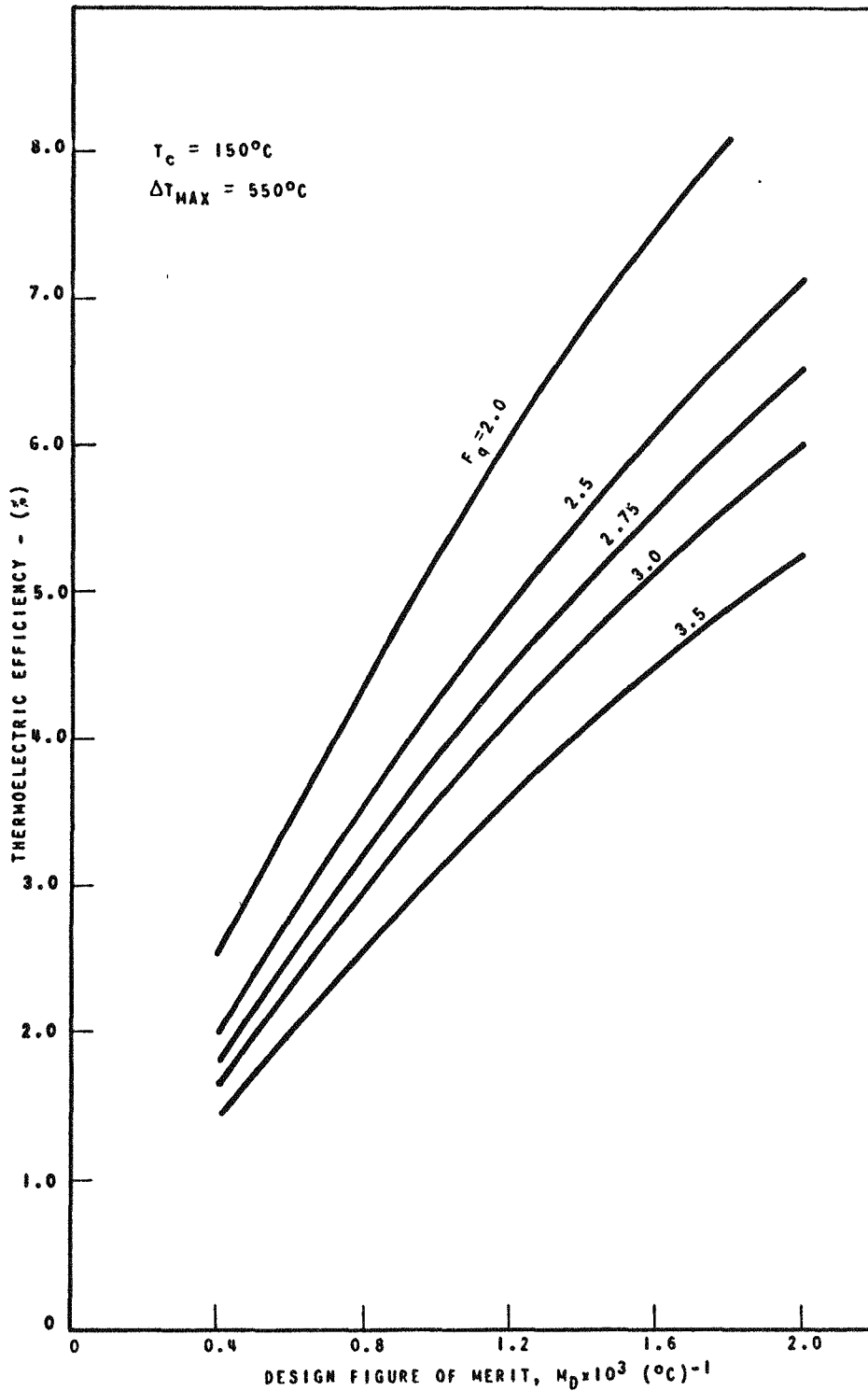


FIGURE 18  
 THERMOELECTRIC REACTOR CORE  
 THERMOELECTRIC EFFICIENCY FOR CASE VIII DESIGN

$K_j$  is the thermoelectric junction thermal conductivity;  $R_j$  is its electrical resistivity; and  $S_j$  is its Seebeck coefficient. The overall core efficiency is defined as the net electrical power output divided by the heat input. The efficiencies do not include utilization of process or space heat. They reflect optimum internal-to-external load ratios (or optimum current flow). They assume negligible contact resistance; a cold junction temperature of  $150^\circ\text{C}$ ; and a  $\Delta T_{\text{max}}$  of  $550^\circ\text{C}$ . Optimized width of P- to N-type elements is considered, using the relationship

$$(1) \quad \left(\frac{L_1}{L_2}\right)^2 = \frac{k_2 \rho_1}{k_1 \rho_2} = \beta$$

where:  $L_1$  = P element width  
 $L_2$  = N element width  
 $k_1$  = P thermal conductivity  
 $k_2$  = N thermal conductivity  
 $\rho_1$  = P electrical resistivity  
 $\rho_2$  = N electrical resistivity

These efficiencies are based on Joule and Peltier heating along with the heat energy transferred by conduction in the thermoelectric element. The design figure of merit,  $Z_D$ , thus turns out to be an optimized (as listed above) combination of the thermoelectric junction's thermal conductivity and electrical resistivity. For the junction design as shown in Figure 17 (see Appendix A for derivation):

$$(2) \quad Z_D = \frac{S_j^2}{K_j R_j} = \frac{A(S_1 + S_2)^2}{k_1 \rho_1 + k_2 \rho_2 + k_1 \rho_2^{1/2} \beta^{1/2} + k_2 \rho_1^{1/2} \beta^{-1/2} + \frac{16.35 \times 10^{-6}}{1 + \beta^{1/2}} \left[ Bk_1 \beta^{1/2} + Ck_2 \right]}$$

where:  $Z_D$  = design figure of merit  
 $S$  = thermoelectric element Seebeck coefficient  
 $k$  = thermoelectric element specific thermal conductivity  
 $\rho$  = thermoelectric element electrical resistivity



subscripts:    1 denotes P-type element  
                   2 denotes N-type element  
                   j denotes total junction

Units to give  $Z_D$  in  $(^{\circ}\text{C})^{-1}$ :

		<u>Value Of</u>		
		<u>A</u>	<u>B</u>	<u>C</u>
Using English Units	$\left\{ \begin{array}{l} S = v/^{\circ}\text{F} \\ \rho = \text{ohm-in} \\ k = \text{Btu/hr-ft-}^{\circ}\text{F} \end{array} \right\}$	73.7	54.2	6.15
Using Metric Units	$\left\{ \begin{array}{l} S = v/^{\circ}\text{C} \\ \rho = \text{ohm-cm} \\ k = \text{watts/cm-}^{\circ}\text{C} \end{array} \right\}$	1.0	137.6	15.7

Design figures of merit of about  $0.0010$  to  $0.0012$   $(^{\circ}\text{C})^{-1}$  are possible utilizing the best presently-obtainable PbTe thermoelectric material. Thus for an  $F_q$  (peak to average core heat flux) of 2.75, overall thermoelectric efficiencies of 4.0 to 4.5 per cent can be attained if identical thermocouple junctions are used throughout the reactor. If a value of  $F_q$  equal to 2.5 could be achieved, efficiencies of 4.3 to 5.0 per cent are predicted. A further reduction in  $F_q$  could further improve these efficiencies. It is reasonable to expect that overall efficiencies in excess of five per cent can be achieved, since in this first calculation, little attempt has been made at optimization through variations in doping and in thermocouple dimensions.

A listing of possible means of optimization (not included in the results presented) should include the following:

1. Variation of thermoelectric element widths and doping throughout the core.

An infinite variation depending on  $\Delta T_{\text{actual}}$ , which in turn affects the junction thermal conductivity and resistivity, would be the optimum case. Possibly the thermoelectric element configuration and doping could be varied by regions throughout the core to improve the performance of the thermoelectric material by effective matching of its properties to the particular temperature ranges.

2. Cascading or staging of elements.

More than one element would be wrapped around the fuel concentrically to better utilize the material properties of the thermoelectric elements.

3. Changing fuel element design.

Since this design is not an optimized case, it should be changed when further information becomes available.

Improved thermoelectric efficiencies should result from efforts to optimize (1) the diameter of the fuel slug, (2) the total junction length, and (3) the thickness of the individual elements with respect to their positions along the length of the fuel rod.

Additional effort should be expended on some of the more feasible items for optimization purposes in the near future.

B. Design

1. Fuel Rod Design

In the sketch of the design adopted for the thermoelectric type fuel rod (Figure 17), the current flow is indicated by the dotted line AB, which may best be described as an axially directed, radially stepped flow path. This element consists of six components:

- (1) the combination fuel matrix slug ( $\text{Fe-UO}_2$  or  $\text{Nb-UO}_2$ ) and inner electrical conductor;
- (2) P- and N-type  $\text{PbTe}$  thermoelectric elements (one P-type and one N-type element form a junction) where net emf is generated due to the radial temperature gradient;
- (3) outer electrical conductor ring of aluminum which connects a P to an N element;
- (4) an annular alumina barrier to (a) insulate the electrical circuit from the outer clad and (b) form a heat barrier so that the required temperature gradient will result between the thermoelectric minimum allowable cold temperature ( $150^\circ\text{C}$ ) and the maximum allowable element surface temperature for a system using aluminum cladding;

- (5) aluminum cladding to cover the alumina;
- (6) staggered insulation (one promising material would be synthetic mica) to obtain the desired electrical circuit as shown by dotted path AB.

$L_1$  and  $L_2$ , the optimized widths of the P- and N-type elements, respectively, are to be adjusted according to the relative properties of the thermoelectric material utilized, per equation (1).

Reasonably good performance should result with the junction width of 0.800 inch. While this value is by no means an optimum (the properties of the thermoelectric material vary considerably over the useful temperature range), it was fixed to simplify the study. For optimum results the individual junction widths throughout the reactor core would be selected for the best match with local temperature conditions. Thus, various values for  $L_1$  and  $L_2$  should also be established throughout the reactor core. Increases in present efficiencies of 10-15 per cent can be accomplished by this type of arrangement (i.e., absolute efficiencies from 4 to 5.75 per cent may be achieved).

Dimensions of the fuel slug and outer aluminum conductor were selected to keep internal electrical losses as low as possible without penalizing other conditions to any great extent. Presently, 0.020 inch appears to be about the minimum feasible insulation thickness. Negligible thermal and electrical contact resistances are assumed.

Assuming five per cent efficiency, approximately 100,000 of these thermoelectric junctions would be required to produce 500 KW power. With a 40 inch long active core, 2000 fuel rods would be required.

From a preliminary thermal analysis, it appears that for this design the peak temperature at the fuel centerline would be 1650°F (900°C).

## 2. Reactor System and Core Design

Figure 19 shows a tentative thermoelectric reactor system utilizing thermal circulation. The coolant flows upward through the core, where heat is absorbed. The heated coolant then rises through the baffles into the heat exchanger for cooling. The cooled water then flows downward in the annular section between the baffles and pressure vessel wall, into the lower plenum around the control rods, and finally enters the core to complete the cycle.

Approximate sizes are given. A "piggy back" type U-tube heat exchanger (minus the steam separation section if hot water is desired) is utilized in this scheme as the cooler from which process or space heat is obtained. The overall size of the reactor is approximately 25 feet long by 74 inches O.D. The core is 53 in. across the flats and has a 40 inch active fuel length. Refueling is accomplished by removing the heat exchanger and upper baffles. Some system parameters are:

- (1) System  $\Delta P$  = thermal driving head - 23.0 psf
- (2) Core to heat exchanger  $\ell$  = 10 ft
- (3) Core flow rate = 450,000 lb/hr
- (4) Core  $\Delta T$  = 75<sup>o</sup>F
- (5) System pressure = 150 psia
- (6) Core exit temperature = 280<sup>o</sup>F

The reactor core design is shown in Figures 20, 21, and 22. Figure 20 is an isometric view illustrating (a) the mechanical arrangement of the parallel-series electric network through the core, and (b) the method of refueling. There are 64 fuel bundles of 32 fuel rods each (Figures 21 and 22). Each block between control rods contains two fuel bundles connected at the top in series by a combination refueling handle and conductor. The plug-in dog-bone-shaped aluminum bottom conductors connect adjacent fuel bundles in series. The arrangement as a whole gives an electrical network of 64 fuel bundles connected in series,

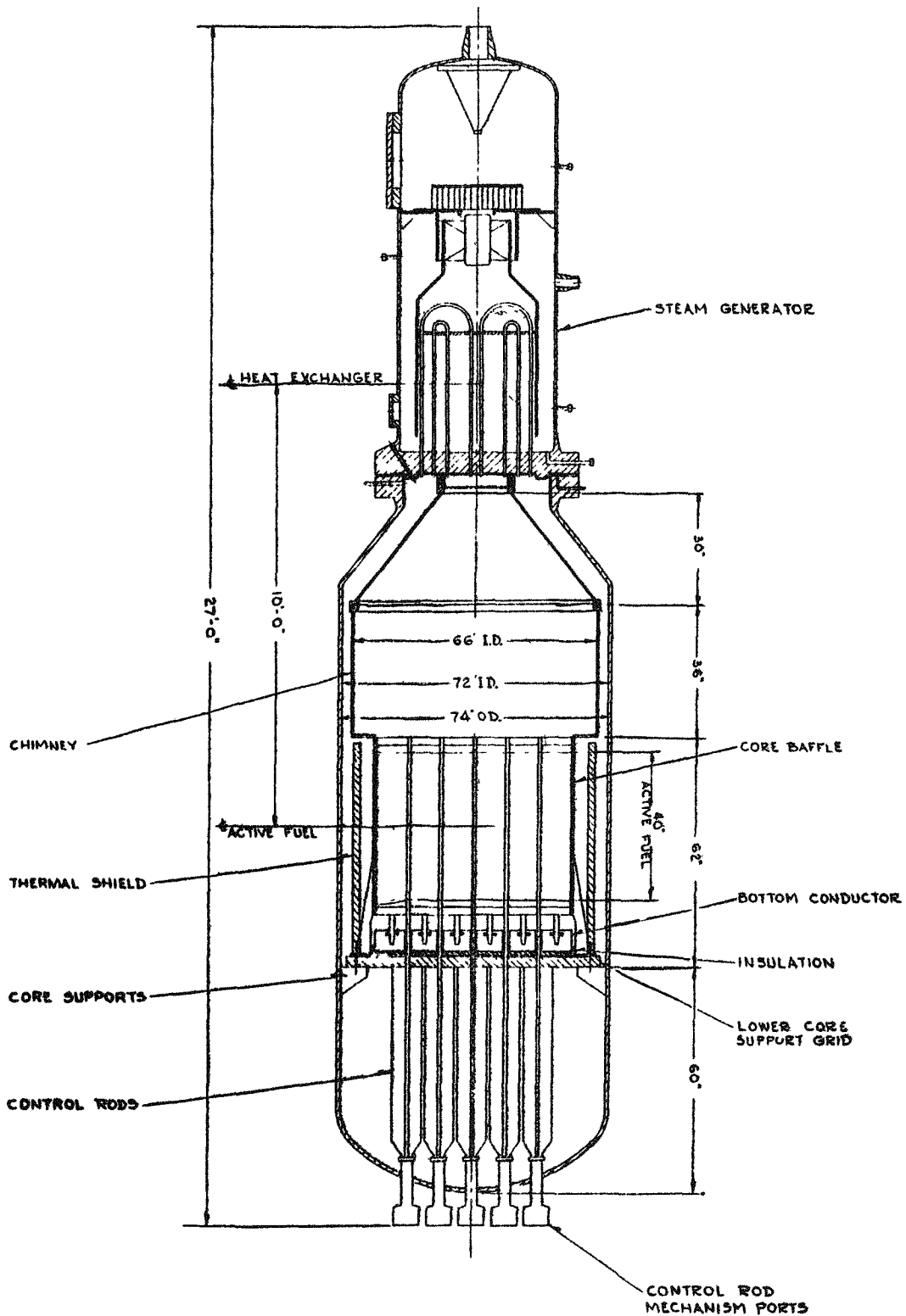
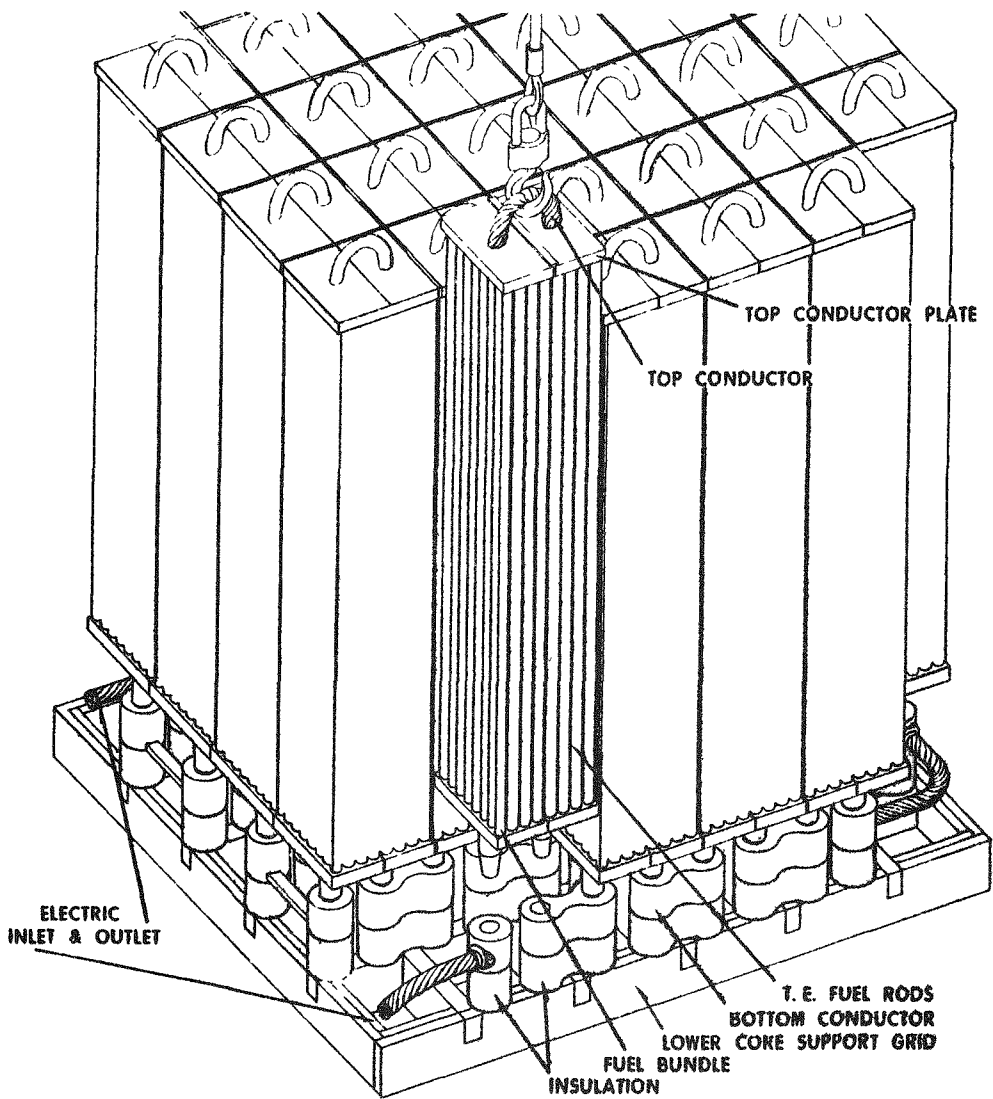


FIGURE 19- THERMOELECTRIC REACTOR SECTIONAL ASSEMBLY



**THERMO - ELECTRIC REACTOR CORE ASSEMBLY**

FIGURE 20

FIGURE 21 - THERMOELECTRIC REACTOR CROSS SECTION

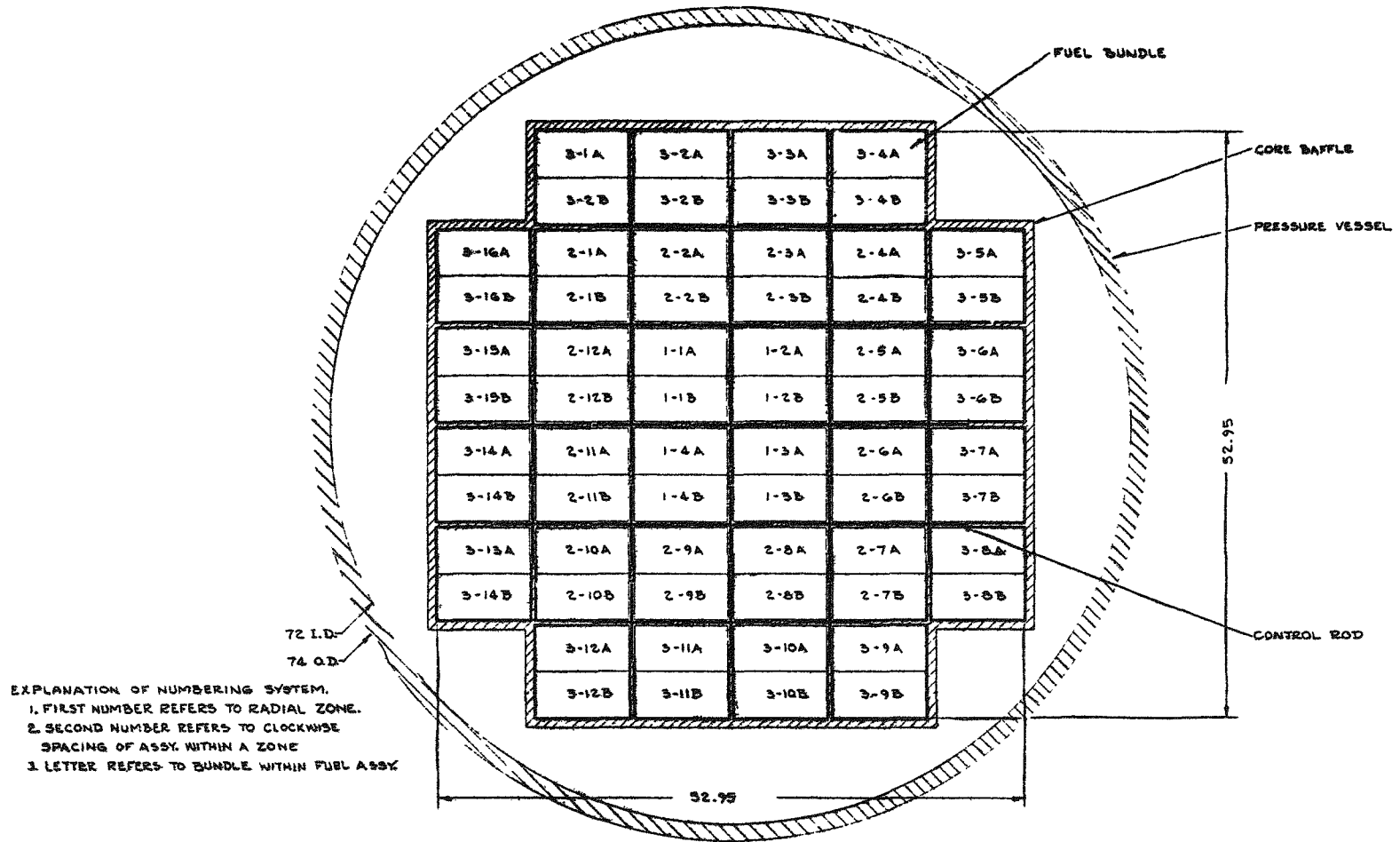
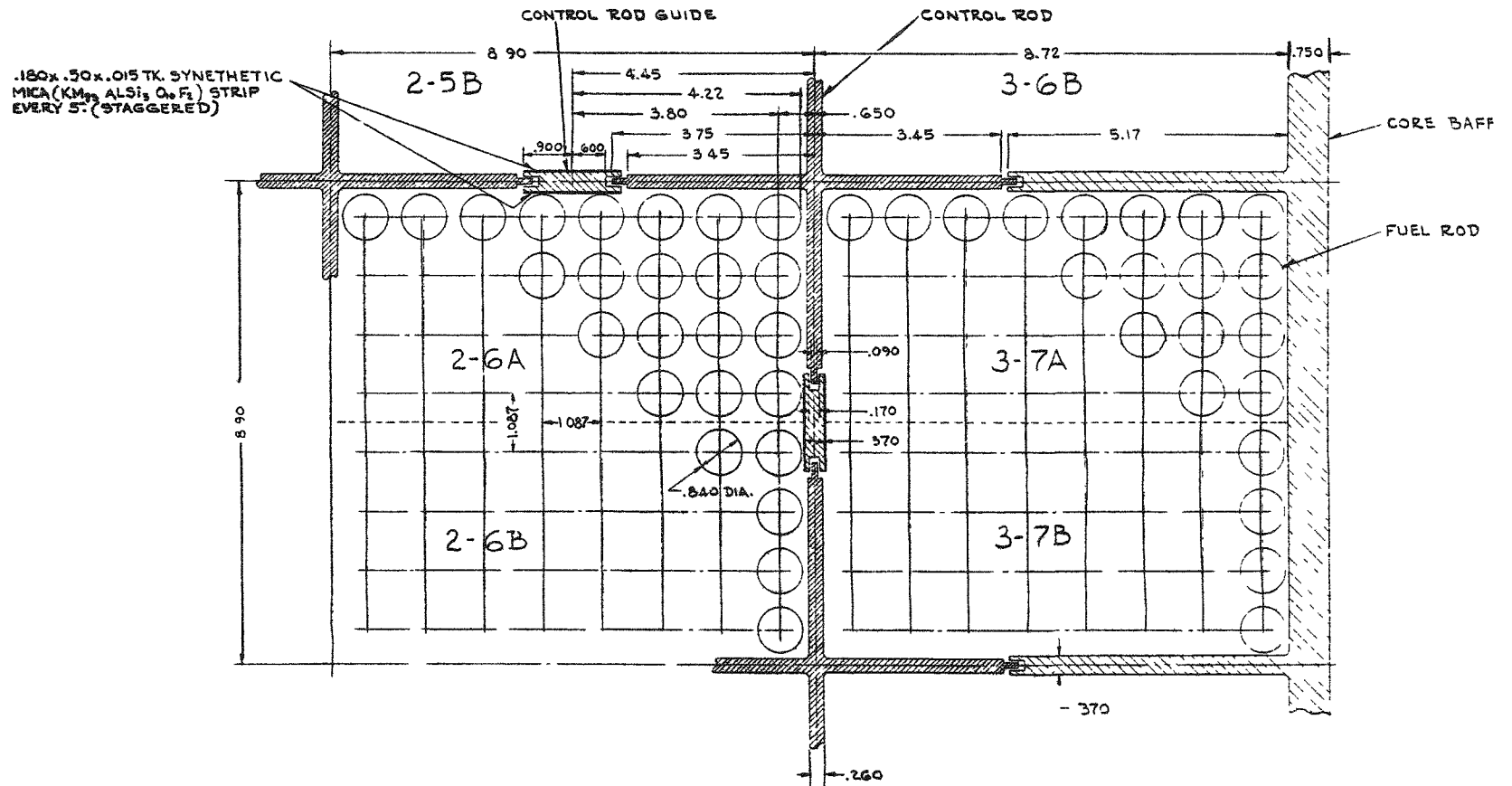


FIGURE 22 - THERMOELECTRIC REACTOR CORE CROSS SECTION





each bundle having 32 parallel electrical paths (fuel rods). This number of parallel paths should afford a reasonable degree of reliability. The fuel rods are connected in parallel by top and bottom aluminum conductor plates which are provided with holes to permit coolant flow. The bottom conductors, and in turn the core, are supported by an egg-crate grid bottom support plate. Insulation is provided between the conductor and the support plate. A grooved 0.370 inch thick aluminum spacer is placed between the fuel bundles as shown in Figure 22 to guide the control rods. If this proves unsatisfactory, a top guide plate can be provided. A fuel rod pitch of 1.087 was dictated by physics considerations.

The core operates at a power density of 6.3 watts/cc, the output being in the neighborhood of 160v-3200amp D.C. Control is afforded by 21 control rods (Figure 21). The optimum number, size, type, and material of these rods need to be determined.

### 3. Nuclear Physics

Preliminary nuclear calculations have been performed on this 500 KW thermoelectric reactor core design. These were hand calculations, except for the lifetime calculations, in which a modified one-group uniform burnup code (CAP-1) was utilized. The cross section values used for tellurium were estimated.

Figure 23 gives the calculated loadings. Certain items of interest are listed in the following tabulation:

<u>Life (years)</u>	<u>U-235 (kg)</u>	
	<u>Fe Fuel Matrix</u>	<u>Nb Fuel Matrix</u>
2 (14,000 fph)	98.5	86
3 (21,000 fph)	104.5	92

An enrichment of 20 a/o U-235 at beginning of life and a vol<sub>H<sub>2</sub>O</sub>/vol<sub>fuel</sub> ratio of 5.0 was used.

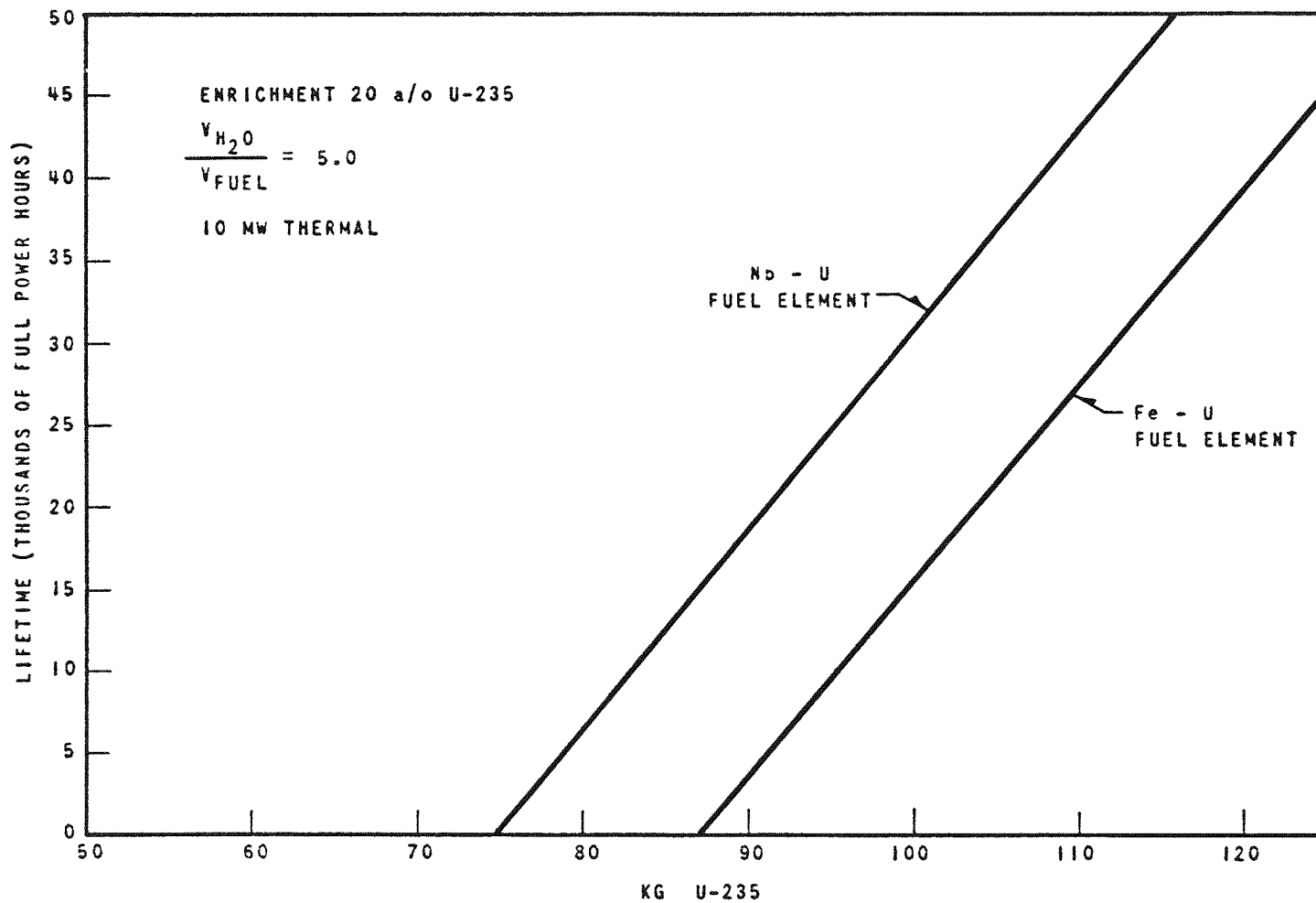


FIGURE 23  
LOADING ESTIMATE FOR THERMOELECTRIC REACTOR

The necessity for extremely high loadings is largely due to (1) the high capture cross-section of tellurium and the matrix material and (2) the wide, open lattice geometry of the core. Since tellurium has an extremely high resonance neutron capture cross-section in the epithermal energy range, it is imperative that a strictly thermal-energy core be achieved. The 1.087 inch pitch appeared to be the optimum fuel rod spacing to accomplish this.

Some definite improvements can be made to reduce these loadings by 50 per cent or more. They are:

- (1) Substitution of BeO as the matrix material. This would require a separate inner conductor since this material is a poor electrical conductor. Although iron is known to be compatible with PbTe at elevated temperatures, its replacement may be advisable because of the high loading factor and because the maximum fuel centerline temperature of 900°C envisaged in the design is very close to the alpha-gamma transformation temperature of the iron.
- (2) As a means of eliminating some of the neutron poison in the core, isotopic separation of the tellurium isotopes is being considered. The highly-undesirable isotope is Te-123, which represents only 0.87 per cent of natural tellurium but accounts for nearly 80 per cent of the thermal absorption and probably 90 per cent of the resonance absorption. Since the abundant and desirable isotopes are Te-126, -128, and -130, elimination of the light isotopes may be feasible.

To estimate the advantage of separating the isotopes, it was assumed that 90 per cent of the Te-123 could be eliminated from natural tellurium. Calculations then indicated that the loading could be reduced by 30-50 kg of U-235 in a core previously containing 100 kg and using natural tellurium. It should be pointed out that the optimum lattice pitch would decrease somewhat if the resonance absorbing isotopes of tellurium were eliminated.

Since the cross-sections of Te-123 and U-235 are comparable, they will deplete in roughly the same fashion. The Te-123 has properties similar to a burnable poison; for long values of core life, a significant fraction of the isotope is burned out. This tends to add reactivity and increase the core life. This effect was not considered in the calculations. It becomes more important in long life cores.

These two improvements are being evaluated.

APPENDIX A

The total internal resistance per thermoelectric junction,

$R_j$  is:

$$(1) \quad R_j = \left( \frac{\rho_1}{A_1} + \frac{\rho_2}{A_2} \right) l + \rho_3 \frac{l_3}{A_3} + \rho_4 \frac{l_4}{A_4}$$

where:

- $\rho_1$  = thermoelectric P element electrical resistivity
- $\rho_2$  = thermoelectric N element electrical resistivity
- $A_1$  = cross sectional area of P element
- $A_2$  = cross sectional area of N element
- $l$  = radial thickness of thermoelectric elements
- $\rho_3$  = electrical resistivity of hot conductor
- $\rho_4$  = electrical resistivity of cold conductor
- $l_3$  = length of electrical flow path in hot conductor
- $l_4$  = length of electrical flow path in cold conductor
- $A_3$  = cross-sectional area of hot conductor
- $A_4$  = cross-sectional area of cold conductor

For design as shown in Figure 18:

$$(2) \quad \left\{ \begin{array}{l} A_1 = \pi D_m L_1 \\ A_2 = \pi D_m L_2 \end{array} \right. \quad \begin{array}{l} A_3 = \frac{\pi D_3^2}{4} \\ A_4 = \frac{\pi}{4(D_o^2 - D_i^2)} \end{array}$$

where:

- $L_1$  = width of P element
- $L_2$  = width of N element
- $D_3$  = O.D. of hot conductor
- $D_o$  = O.D. of cold conductor
- $D_i$  = I.D. of cold conductor
- $D_m$  = mean diameter of thermoelectric elements

Approximating the electrical flow path of the hot conductor,

$l_3$  is:

$$(3) \quad l_3 = \frac{L_1 + L_2}{2} + L_i + S$$

where:  $L_i$  = width of insulation

$S$  = electrical flow path compensating factor

The total junction length  $L$  is

$$(4) \quad L = L_1 + L_2 + 2L_i \quad \text{where} \quad L_i = \text{width of insulation}$$

Then (3) becomes

$$(5) \quad l_3 = \frac{L}{2} + S$$

The approximate path of electrical flow of  $l_4$  is

$$(6) \quad l_4 = \frac{L_1 + L_2}{2} + L_i$$

$$(7) \quad l_4 = \frac{L}{2}$$

Combining (2), (5), and (6) into (1),

$$(8) \quad R_j = \left( \frac{\rho_1}{L_1} + \frac{\rho_2}{L_2} \right) \frac{1}{\pi D_m} + \rho_3 \frac{\frac{L}{2} + S}{A_3} + \rho_4 \frac{\frac{L}{2}}{A_4}$$

A close approximation of the thermal conductance of the junction  $K$  is

$$(9) \quad K = \left( k_1 L_1 + k_2 L_2 \right) \frac{\pi D_m}{1}$$

where:  $k_1$  = specific thermal conductivity of P element

$k_2$  = specific thermal conductivity of N element

Also, using Ioffe's relationship for optimum electrical flow cross-sectional areas when the length of the thermoelement is held constant,

$$(10) \quad \left(\frac{L_1}{L_2}\right)^2 = \frac{k_2 \rho_1}{k_1 \rho_2} = \beta$$

or

$$(11) \quad L_1 = L_2 \beta^{1/2}$$

Using equations (4) and (11)

$$(12) \quad L_2 = \frac{L - 2L_1}{1 + \beta^{1/2}}$$

and

$$(13) \quad L_1 = \frac{(L - 2L_1) \beta^{1/2}}{1 + \beta^{1/2}}$$

Substituting (12) and (13) into (8) and (9) and multiplying (8) and (9), thus eliminating individual lengths of each thermoelectric element which are a function of the properties, we obtain:

(14)

$$(K_j R_j)_{\text{opt}} = k_1 \rho_1 + k_2 \rho_2 + k_1 \rho_2 \beta^{1/2} + k_2 \rho_1 \beta^{-1/2} + \frac{\pi D_m}{L(1 + \beta^{1/2})} \left[ k_1 \rho_3 \frac{(L - 2L_1) \beta^{1/2} \left(\frac{L}{2} + S\right)}{A_3} + k_2 \rho_4 \frac{L(L - 2L_1)}{2A_4} \right]$$

Substituting in (14) the values:

$$\begin{aligned} l &= 0.100 \text{ inch} = 0.0833 \text{ feet} = 0.254 \text{ cm} \\ L &= 0.800 \text{ inch} = 0.667 \text{ feet} = 2.032 \text{ cm} \\ D_m &= 0.520 \text{ inch} = 0.0433 \text{ feet} = 1.32 \text{ cm} \\ S &= 0.060 \text{ inch} = 0.1523 \text{ cm} \\ L_1 &= 0.020 \text{ inch} = 0.0508 \text{ cm} \\ A_3 &= 0.1256 \text{ in}^2 = 0.810 \text{ cm}^2 \\ A_4 &= 0.1022 \text{ in}^2 = 0.660 \text{ cm}^2 \\ \rho_3 &= 19.5 \times 10^{-6} \text{ ohm-in} = 49.5 \times 10^{-6} \text{ ohm-cm} \\ \rho_4 &= 2.08 \times 10^{-6} \text{ ohm-in} = 5.28 \times 10^{-6} \text{ ohm-cm} \end{aligned}$$

we obtain

$$(15) \quad (K_{jR_j})_{opt} = k_1 \rho_1 + k_2 \rho_2 + k_1 \rho_2 \beta^{1/2} + k_2 \rho_1 \beta^{-1/2} + \frac{16.35 \times 10^{-6}}{1 + \beta^{1/2}} \left[ Bk_1 \beta^{1/2} + Ck_2 \right]$$

and, to obtain the junction design figure of merit;  $Z_D$ ,

$$(16) \quad Z_D = \frac{S_j^2}{(K_{jR_j})_{opt}}$$

where  $S_j = S_1 + S_2 =$  the junction thermoelectric element Seebeck coefficient

Combining (15) into (16) will give us an optimized  $Z_D$ , or

$$(17) \quad Z_D = \frac{A(S_1 + S_2)^2}{k_1 \rho_1 + k_2 \rho_2 + k_1 \rho_2 \beta^{1/2} + k_2 \rho_1 \beta^{-1/2} + \frac{16.35 \times 10^{-6}}{1 + \beta^{1/2}} \left[ Bk_1 \beta^{1/2} + Ck_2 \right]}$$

where A arises when converting from metric units to English units.

To obtain  $Z_D$  in  $(^\circ\text{C})^{-1}$  :

		<u>Value of</u>		
		<u>A</u>	<u>B</u>	<u>C</u>
Using English Units	$\left\{ \begin{array}{l} S = \text{v}/^\circ\text{F} \\ \rho = \text{ohm-in} \\ k = \text{Btu/hr-ft-}^\circ\text{F} \end{array} \right\}$	73.7	54.2	6.15
Using Metric Units	$\left\{ \begin{array}{l} S = \text{v}/^\circ\text{C} \\ \rho = \text{ohm-cm} \\ k = \text{watts/cm-}^\circ\text{C} \end{array} \right\}$	1.0	137.6	15.7